

Entanglement in solvable many-particle models

Ingo Peschel

Fachbereich Physik, Freie Universität Berlin, Arnimallee 14, D-14195 Berlin,
Germany

Abstract.

Lecture notes for the Brazilian School on Statistical Mechanics
Natal, Brazil, July 18-22, 2011.

The five lectures introduce to the description of entanglement in many-particle systems and review the ground-state entanglement features of standard solvable lattice models. This is done using a thermodynamic formulation in which the eigenvalue spectrum of a certain Hamiltonian determines the entanglement properties. The methods to obtain it are discussed and results, both analytical and numerical, for various cases including time evolution are presented.

Preface

Entanglement in many-particle quantum states has been a topic of intense research in recent years with applications in numerics and interesting links to statistical physics. It is therefore excellently suited for an advanced course in a summer school. The following notes correspond closely to five lectures given in July 2011 at the International Institute of Physics in Natal, Brazil. They are based on a recent review article [1], but the material has been properly adapted to the purpose. Thus they contain more introductory examples and certain topics are presented in more detail. On the other hand, new material from the last two years, as well as supplementary notes have been added. Throughout the notes, the style is lecture-like with itemized statements. References are only given in direct connection with the problem at hand, show a preference of own work and should not be regarded as an exhaustive list. Compared to the version handed out in Natal, additional figures have been included and some editing took place.

Contents

1. Background and basics
2. Free-particle models
3. Integrable models
4. Entanglement entropies
5. Quenches and miscellaneous

1. Background and basics

In this section, I summarize the basic features of entangled states and reduced density matrices and illustrate them with examples. For further details, see e.g. the short review [2].

1.1. Introduction

Entanglement is a notion which goes back to 1935 when it was introduced by Schrödinger in a series of three articles (in German, the German word is “Verschränkung”) [3]. At the same time Einstein, Podolski and Rosen discussed their famous “Gedankenexperiment”, in which they considered two particles with fixed total momentum and relative distance. Nowadays this is usually formulated with two spins, and this is also where one encounters entanglement first. Entanglement has to do with the features of quantum states and the information contained in wave functions. For a long time, it was a topic discussed mostly in quantum optics and for systems with few degrees of freedom.

In the last 25 years, however, it has seen a revival with input from very different areas, namely

- the theory of black holes
- the numerical investigation of quantum chains
- the field of quantum information

In these cases one always deals with large systems and many degrees of freedom.

In entanglement investigations, one asks the following *question*:

- given a total system in a certain quantum state $|\Psi\rangle$
- divide it (in space, or in Hilbert space) in two parts (bipartition)
- how are the two parts coupled in $|\Psi\rangle$?

This is more general than looking at, say, a two-point correlation function. And there is a general way to answer this question, namely one can bring $|\Psi\rangle$ into a standard form, which displays the coupling. This is the *Schmidt decomposition* which we will discuss in a moment. To obtain it in practice, one uses quantities which determine all properties of a subsystem, namely *reduced density matrices* (RDMs). They also contain the information on the entanglement and will be the basic *tool* throughout the lectures.

The *states* we will study are the ground states of models which, on the one hand, are solvable and, on the other hand, have a physical significance, like tight-binding (hopping) models or spin chains. As in other contexts, they serve as points of orientation which allow to study the features of the problem and to develop a feeling and an overall picture. My own interest arose in connection with the DMRG, where the entanglement turned out to be crucial for the performance of the method. Entanglement continues to play a role also in other algorithms and their design, and in this respect it has quite practical implications. But in these lectures, we shall be concerned essentially with the theory.

1.2. Schmidt decomposition

Consider a quantum system in state $|\Psi\rangle$ and divide it into two parts 1 and 2. Then one can write

$$|\Psi\rangle = \sum_{m,n} A_{m,n} |\Psi_m^1\rangle |\Psi_n^2\rangle \quad (1)$$

where the $|\Psi_m^1\rangle$ and $|\Psi_n^2\rangle$ are orthonormal bases in the two Hilbert spaces.

Note that one has a double sum and that the matrix $A_{m,n}$ is in general rectangular, since the dimensions of the Hilbert spaces can differ. Nevertheless one can obtain a diagonal form via the so-called singular-value decomposition

$$\mathbf{A} = \mathbf{U}\mathbf{D}\mathbf{V}' \quad (2)$$

where \mathbf{U} is square and unitary, \mathbf{D} diagonal and \mathbf{V}' rectangular with orthonormal rows. This gives

$$|\Psi\rangle = \sum_{m,n,k} U_{m,n} D_{n,n} V'_{n,k} |\Psi_m^1\rangle |\Psi_k^2\rangle \quad (3)$$

Combining $|\Psi_m^1\rangle$ with \mathbf{U} and $|\Psi_k^2\rangle$ with \mathbf{V}' one obtains with $\lambda_n = D_{n,n}$

$$|\Psi\rangle = \sum_n \lambda_n |\Phi_n^1\rangle |\Phi_n^2\rangle \quad (4)$$

This is called the Schmidt decomposition (Schmidt 1907) [4]. For the history see section 1.7. It has the following features

- Single sum, limited by the smaller Hilbert space
- New orthonormal sets $|\Phi_n^\alpha\rangle$ in both parts
- $\sum |\lambda_n|^2 = 1$ if $|\Psi\rangle$ is normalized
- Entanglement encoded in the λ_n
- Limiting cases
 - $\lambda_1 = 1, \lambda_n = 0$ for $n > 1$: only one term, product state, no entanglement
 - $\lambda_n = \lambda$ for all n : all terms equal weight, maximal entanglement

This refers to a particular bipartition and one can investigate different partitions to obtain a complete picture. Some standard bipartitions for one-dimensional systems are shown in fig. 1.

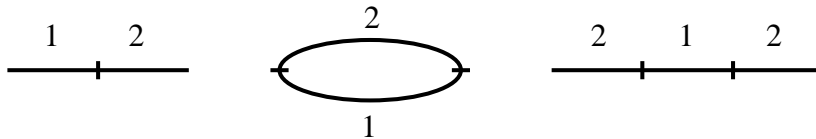


Figure 1. Bipartitions: Chain cut in two halves (left), ring cut in two halves (centre) and segment in an infinite chain (right).

1.3. Examples

We give here examples for the Schmidt decomposition in three different systems.

(a) *Two spins one-half*

$$|\Psi_1\rangle = |+\rangle|+\rangle \quad \text{product state} \quad (5)$$

$$\begin{aligned} |\Psi_2\rangle &= a|+\rangle|+\rangle + b|+\rangle|-\rangle \\ &= |+\rangle \left[a|+\rangle + b|-\rangle \right] \quad \text{product state} \end{aligned} \quad (6)$$

$$|\Psi_3\rangle = a|+\rangle|+\rangle + d|-\rangle|-\rangle \quad \text{entangled state} \quad (7)$$

All these states are already in Schmidt form. However

$$\begin{aligned} |\Psi_4\rangle &= a|+\rangle|+\rangle + b|+\rangle|-\rangle + c|-\rangle|+\rangle \\ &= |+\rangle \left[a|+\rangle + b|-\rangle \right] + c|-\rangle|+\rangle \end{aligned} \quad (8)$$

is entangled, but not in Schmidt form, because the two states in subsystem 2 are not orthogonal.

(b) *Two large spins* [6]

Consider the ferromagnetic spin one-half Heisenberg chain with N sites

$$H = -J \sum_n \mathbf{s}_n \mathbf{s}_{n+1} \quad (9)$$

All eigenstates can be written as $|\Psi\rangle = |S, S^z\rangle$ with total spin S and z -component S^z . In the ground state all spins are parallel, $S = N/2$, and S^z can be chosen. Choose $S^z = 0$ and divide the chain in two halves. Then one can use angular momentum addition as illustrated in fig. 2

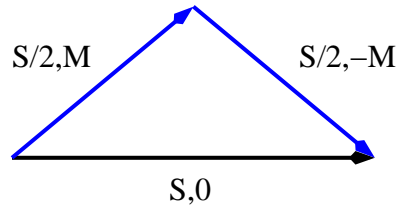


Figure 2. The state $|S, 0\rangle$ obtained from states in the subsystem.

to obtain

$$|S, 0\rangle = \sum_{M=-S/2}^{S/2} c_M |S/2, M\rangle_1 |S/2, -M\rangle_2 \quad (10)$$

with the Clebsch-Gordan coefficients

$$c_m = \frac{S!}{\sqrt{(2S)!}} \frac{S!}{(S/2 - M)!(S/2 + M)!} \quad (11)$$

This is the Schmidt form for this state. Its features are

- Only (S+1) terms, while dimension of Hilbert space is 2^S
- For large S , $c_M \sim \exp(-2M^2/S)$, Gaussian
- Analogous formulae for arbitrary S^z
- Special case $S^z = S$, all spins in the z -direction. Then $|S, S\rangle$ is a product state

$$|S, S\rangle = |S/2, S/2\rangle_1 |S/2, S/2\rangle_2 \quad (12)$$

(c) *Two coupled oscillators* [7]

Consider the Hamiltonian ($m = \hbar = 1$)

$$H = \frac{1}{2}(p_1^2 + \omega_0^2 x_1^2) + \frac{1}{2}(p_2^2 + \omega_0^2 x_2^2) + \frac{1}{2}k(x_1 - x_2)^2 \quad (13)$$

The eigenfrequencies are $\omega_1^2 = \omega_0^2 + 2k$ and $\omega_2^2 = \omega_0^2$ with corresponding normal coordinates

$$y_1 = \frac{1}{\sqrt{2}}(x_1 - x_2), \quad y_2 = \frac{1}{\sqrt{2}}(x_1 + x_2) \quad (14)$$

In these coordinates, the ground state is the product of two Gaussians

$$|\Psi_0\rangle = \left(\frac{\omega_1 \omega_2}{\pi^2}\right)^{1/4} \exp\left(-\frac{1}{2}[\omega_1 y_1^2 + \omega_2 y_2^2]\right) \quad (15)$$

Then the following formula holds

$$|\Psi_0\rangle = \sum_{n=0}^{\infty} \frac{(-\tanh \eta)^n}{\cosh \eta} |\Phi_n(x_1)\rangle |\Phi_n(x_2)\rangle \quad (16)$$

where $\exp(4\eta) = \omega_1/\omega_2$ and the $|\Phi_n\rangle$ are oscillator states for a frequency $\bar{\omega} = \sqrt{\omega_1 \omega_2}$, i.e. in between ω_1 and ω_2 .

Features

- Schmidt states are “squeezed” states
- Coefficients decay exponentially, $\lambda_n^2 \sim \exp(-\varepsilon n)$
- weak coupling k : $\omega_1 \approx \omega_2 \rightarrow \eta$ small, ε large, rapid decay, weak entanglement
- strong coupling k : $\omega_1 \gg \omega_2 \rightarrow \eta$ large, ε small, slow decay, strong entanglement

These features are also found for one oscillator in a whole assembly.

1.4. Reduced density matrices

The Schmidt structure just discussed can be found from the density matrices associated with the state $|\Psi\rangle$. This is also the standard way to obtain it. Starting from the total density matrix

$$\rho = |\Psi\rangle\langle\Psi| \quad (17)$$

one can, for a chosen division, take the trace over the degrees of freedom in one part of the system. This gives the reduced density matrix for the other part, i.e.

$$\rho_1 = \text{tr}_2(\rho) \quad , \quad \rho_2 = \text{tr}_1(\rho) \quad (18)$$

These hermitian operators can be used to calculate arbitrary expectation values in the subsystems. As to the entanglement, assume that $|\Psi\rangle$ has the Schmidt form (4). Then

$$\rho = |\Psi\rangle\langle\Psi| = \sum_{n,n'} \lambda_n \lambda_{n'}^* |\Phi_n^1\rangle\langle\Phi_n^2| \langle\Phi_{n'}^1| \langle\Phi_{n'}^2| \quad (19)$$

Taking the traces with the $|\Phi_n^\alpha\rangle$ gives $n' = n$ and

$$\rho_\alpha = \sum_n |\lambda_n|^2 |\Phi_n^\alpha\rangle\langle\Phi_n^\alpha| \quad , \quad \alpha = 1, 2 \quad (20)$$

This means that

- ρ_1 and ρ_2 have the same non-zero eigenvalues
- these eigenvalues are given by $w_n = |\lambda_n|^2$
- their eigenfunctions are the Schmidt functions $|\Phi_n^\alpha\rangle$

Therefore the eigenvalue spectrum of the ρ_α gives directly the weights in the Schmidt decomposition and a glance at this spectrum shows the basic entanglement features of the state, for the chosen bipartition. For this reason, it has also been termed “entanglement spectrum” [8].

Remarks

- the ρ_α describe mixed states. An expectation value in subsystem α is given by

$$\langle A_\alpha \rangle = \sum_n |\lambda_n|^2 \langle \Phi_n^\alpha | A_\alpha | \Phi_n^\alpha \rangle \quad (21)$$

- Since the ρ_α are hermitian and have non-negative eigenvalues, one can write

$$\rho_\alpha = \frac{1}{Z} e^{-\mathcal{H}_\alpha} \quad (22)$$

where Z is a normalization constant and the operator \mathcal{H}_α has been termed “entanglement Hamiltonian”. This form will be encountered permanently in the following.

- The ρ_α should not be confused with e.g. the one-particle density matrices, which are simple correlation functions.

Usually, one starts in a basis where $|\Psi\rangle$ has the form (1). Then

$$\rho = |\Psi\rangle\langle\Psi| = \sum_{m,n,m',n'} A_{m,n} A_{m',n'}^* |\Psi_m^1\rangle\langle\Psi_n^2| \langle\Psi_{m'}^1| \langle\Psi_{n'}^2| \quad (23)$$

and taking the trace with the $|\Psi_n^2\rangle$ gives $n' = n$ and

$$\rho_1 = \sum_{m,m'} \sum_n A_{m,n} A_{n,m'}^\dagger |\Psi_m^1\rangle\langle\Psi_{m'}^1| \quad (24)$$

Thus ρ_1 contains the square hermitian matrix $\mathbf{A}\mathbf{A}^\dagger$ and similarly ρ_2 contains $(\mathbf{A}^\dagger\mathbf{A})^*$. The form (20) is then obtained by diagonalizing these matrices. This is the general approach.

Example: Two spins one-half

A general normalized state is

$$|\Psi\rangle = a|+\rangle|+\rangle + b|+\rangle|-\rangle + c|-\rangle|+\rangle + d|-\rangle|-\rangle \quad (25)$$

where $|a|^2 + |b|^2 + |c|^2 + |d|^2 = 1$. The matrix \mathbf{A} is then

$$\mathbf{A} = \begin{pmatrix} a & b \\ c & d \end{pmatrix} \quad (26)$$

and one obtains

$$\mathbf{A}\mathbf{A}^\dagger = \begin{pmatrix} aa^* + bb^* & ac^* + bd^* \\ ca^* + bd^* & cc^* + dd^* \end{pmatrix} \quad (27)$$

Since the trace is one, the eigenvalues are given by

$$w_{1,2} = \frac{1}{2} \pm \sqrt{\frac{1}{4} - \det(\mathbf{A}\mathbf{A}^\dagger)} \quad (28)$$

The state is entangled if $w_{1,2} \neq 0, 1$, i.e. if $\det\mathbf{A} = ad - bc \neq 0$. This includes the state $|\Psi_4\rangle$ in section 1.3, where $a, b, c \neq 0$ and $d = 0$.

1.5. Application: DMRG

The density-matrix renormalization group method (DMRG) is a numerical procedure, which was introduced by Steven White in 1992 [9, 10] and makes direct use of the Schmidt decomposition and the reduced density matrices. For a review, see [11].

Consider a quantum chain, e.g. a spin one-half model, with open ends. Then in the simplest variant, the following steps take place, compare fig. 3.

(0) Start

Begin with a small system of 5-10 sites.

Calculate the ground state *exactly*.

(1) Schmidt decomposition

Divide into two halves.

Calculate the RDM's.

Diagonalize them and obtain the Schmidt coefficients and Schmidt states.

(2) Approximation

Keep only the m Schmidt states with largest weights w_n .

Truncation error: sum of the discarded weights $\sum_{n>m} w_n$.

(3) Enlargement

Insert (two) additional sites in the center.

Form new Hamiltonian in the basis of kept and additional states.

Calculate ground state.

Go back to (1) and repeat.

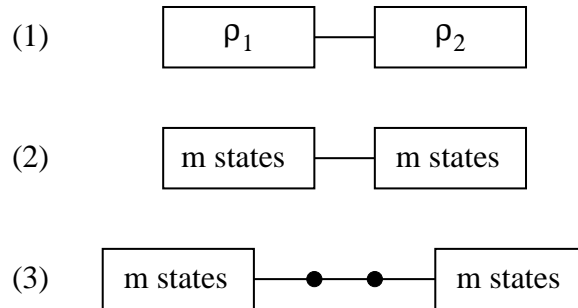


Figure 3. Steps in the (infinite-size) DMRG algorithm.

For this procedure, the form of the Schmidt spectra is crucial. To have a good performance, a rapid drop of the w_n is necessary such that only a small number of Schmidt states has to be kept. In terms of entanglement, the state must be *weakly entangled*. This is satisfied for non-critical chains. For an Ising model in a transverse field, such a small number as 16 Schmidt states gives already a fantastic accuracy for the ground-state energy. It is therefore important to understand the features of RDM spectra and this leads directly to the study of solvable cases, which is the topic of these lectures.

1.6. Entanglement entropy

The full RDM spectra give the clearest impression of the entanglement in a bipartite system. But it is also desirable to have a simple measure through one number. Since the eigenvalues of the RDM's can be viewed as probabilities, one can take the usual entropy, as used in probability theory, to characterize the w_n . This gives the (von Neumann) entanglement entropy

$$S_\alpha = -\text{tr}(\rho_\alpha \ln \rho_\alpha) = -\sum_n w_n \ln w_n, \quad (29)$$

which is the common entanglement measure for bipartitions. It has the following properties

- $S_1 = S_2 \equiv S$ since the spectra are equal. One can talk of *the* entanglement entropy.
- $S = 0$ for product states.
- S is maximal if all w_n are equal.

If $w_n = 1/M$ for $n = 1, 2, \dots, M$ then $S = \ln M$.

The last property leads to a simple interpretation of S . Write

$$S = \ln M_{\text{eff}} \quad (30)$$

Then e^S is an effective number of states in the Schmidt decomposition.

A related measure is the Rényi entropy

$$S_n = \frac{1}{1-n} \ln \text{tr}(\rho_\alpha^n) \quad (31)$$

where n can also be non-integer. S_n has similar properties as S and the same extremal values $S = 0$ and $S = \ln M$. For $n \rightarrow 1$ write

$$S_n = \frac{1}{1-n} \ln \text{tr}[\rho_\alpha \exp((n-1) \ln \rho_\alpha)] \quad (32)$$

and expand the exponential function to obtain $S_1 = S$. The Rényi entropy is somewhat simpler to calculate, since it contains only a power of ρ_α . The important point is that both entropies measure a *mutual connection* and will, in general, *not* be proportional to the size of a subsystem as usual thermodynamic entropies are.

1.7. Historical note

Erhard Schmidt (1876-1959) obtained his PhD in 1905 with Hilbert in Göttingen and was professor at the Berlin university 1917-1950. He is most widely known by the orthogonalization procedure bearing his name. The work linking him to the quantum problems discussed here, appeared in 1907 in the prestigious journal “Mathematische Annalen” [4]. It was based on his thesis and dealt with coupled integral equations with a non-symmetric kernel $K(s, t)$.

In abstract notation, and changing his parameter λ to $1/\lambda$, the equations were

$$K\psi = \lambda\phi, \quad K'\phi = \lambda\psi \quad (33)$$

He deduced a spectral representation for K

$$K(s, t) = \sum_n \lambda_n \phi_n(s) \psi_n(t) \quad (34)$$

where ϕ_n and ψ_n are the eigenfunctions of the symmetric kernels KK' and $K'K$ with common eigenvalue λ_n^2

$$KK'\phi_n = \lambda_n^2 \phi_n, \quad K'K\psi_n = \lambda_n^2 \psi_n \quad (35)$$

One sees that the kernel $K(s, t)$ corresponds to the total wave function, which for two degrees of freedom is $\Psi(x_1, x_2)$. Moreover, one sees that he already worked with the quantities which in the present context are called reduced density matrices. And finally, he discussed best approximations for the kernel based on keeping the terms with largest weights, which is the same recipe as used in the DMRG.

The representation of a wave function $\Psi(x_1, x_2)$ in this way was discussed in a paper by Schrödinger in 1935 [5]. At that time, unsymmetric kernels were already well-known in mathematics, so he referred not to Schmidt but to the textbook by Courant and Hilbert. The specialists will notice that the equations (33), (35) with $K = A - B$ and $K' = A + B$ are just the ones appearing in the famous paper by Lieb, Schultz and Mattis (1961) [12] where they diagonalize a quadratic form in fermions.

2. Free-particle models

2.1. Solvable cases

Before we start the discussion of the free-particle models, which will be the focus of these lectures, let me list the quantum states for which one can obtain explicit results for bipartite RDM's and thus for the entanglement

- Ground states of free-fermion or free-boson systems
- Ground states of certain integrable models
- Ground states of conformally invariant models
- Ground states which have matrix-product form or other simple structures

An example of the last case was the ferromagnetic ground state in section 1.3.

2.2. Free particles, general result

Consider models where the Hamiltonian is a quadratic form in fermionic or bosonic operators and defined on a lattice. Two standard examples are

- Fermionic hopping models with conserved particle number

$$H = -\frac{1}{2} \sum_{m,n} t_{m,n} c_m^\dagger c_n \quad (36)$$

- Coupled oscillators with eigenfrequency ω_0

$$H = \sum_n \left[-\frac{1}{2} \frac{\partial^2}{\partial x_n^2} + \frac{1}{2} \omega_0^2 x_n^2 \right] + \frac{1}{4} \sum_{m,n} k_{m,n} (x_m - x_n)^2 \quad (37)$$

For such free-particle models, the reduced density matrices for the ground state can be written

$$\rho_\alpha = \frac{1}{Z} e^{-\mathcal{H}_\alpha}, \quad \mathcal{H}_\alpha = \sum_{l=1}^L \varepsilon_l f_l^\dagger f_l \quad (38)$$

Here L is the number of sites in subsystem α and the operators f_l^\dagger, f_l are fermionic or bosonic creation and annihilation operators for single-particle states with eigenvalues ε_l . The f 's are related to the original operators in the subsystem by a canonical transformation. The constant Z ensures the correct normalization $\text{tr}(\rho_\alpha) = 1$.

Note the following features

- ρ_α looks thermodynamic.
- the “entanglement Hamiltonian” \mathcal{H}_α is of the *same type* as H .

We will see later that \mathcal{H}_α is not the Hamiltonian of the subsystem. Therefore (38) is not a true Boltzmann formula. Nevertheless, the entanglement problem has been reduced to that of a certain Hamiltonian and its thermodynamic properties. But first we want to derive the result.

2.3. Method 1 - Direct approach

The direct method to obtain ρ_α is to integrate over the degrees of freedom outside the subsystem α . We illustrate it for the example of two oscillators discussed already in section 1.3 [13]. The ground state was

$$|\Psi_0\rangle = \left(\frac{\omega_1\omega_2}{\pi^2}\right)^{1/4} \exp\left(-\frac{1}{2}[\omega_1 y_1^2 + \omega_2 y_2^2]\right) \quad (39)$$

One goes through the following steps.

Step I

- Write in terms of x_1 and x_2
- Form $|\Psi_0\rangle\langle\Psi_0|$, i.e. $\Psi_0(x_1, x_2)\Psi_0(x'_1, x'_2)$
- Set $x'_2 = x_2$ and integrate over x_2
- Use $(x_1 + x'_1)^2 = 2(x_1^2 + x'^2_1) - (x_1 - x'_1)^2$
- Result

$$\rho_1(x_1, x'_1) = C \exp\left(-\frac{1}{2}(a-b)x_1^2\right) \exp\left(-\frac{b}{4}(x_1 - x'_1)^2\right) \exp\left(-\frac{1}{2}(a-b)x'^2_1\right) \quad (40)$$

where $a = (\omega_1 + \omega_2)/2$ and $b = (\omega_1 - \omega_2)^2/2(\omega_1 + \omega_2)$.

Due to the derivation, ρ_1 has the form of an integral operator. To obtain its eigenfunctions and eigenvalues, one would have to solve an integral equation.

Step II

- Determine the differential operator for which (40) is the (x_1, x'_1) matrix element.
- Observe that

$$\exp\left(-\frac{b}{4}(x_1 - x'_1)^2\right) = 2\left(\frac{\pi}{b}\right)^{1/2} \langle x_1 | \exp\left(\frac{1}{b} \frac{\partial^2}{\partial x_1^2}\right) | x'_1 \rangle \quad (41)$$

Proof: Express the operator on the right in terms of its eigenfunctions $\psi_k(x) = (2\pi)^{-1/2} \exp(ikx)$ and integrate over k

- Introduce new coordinates $y^2 = bx_1^2/2$ and the frequency $\omega^2/4 = (a-b)/b$
- Result

$$\rho_1 = K \exp\left(-\frac{1}{4}\omega^2 y^2\right) \exp\left(\frac{1}{2} \frac{\partial^2}{\partial y^2}\right) \exp\left(-\frac{1}{4}\omega^2 y^2\right) \quad (42)$$

If one could simply pull the exponentials together, one would have the Hamiltonian of a harmonic oscillator in the exponent. However, the exponentials do not commute.

Step III

- Write in terms of boson operators α, α^\dagger where $\alpha = \sqrt{\omega/2}(y + 1/\omega \partial/\partial y)$
- Set up equations of motion for Heisenberg operators of α, α^\dagger formed with ρ_1
- Find Bogoliubov transformation to new boson operators β, β^\dagger

$$\beta = \text{ch}\theta \alpha + \text{sh}\theta \alpha^\dagger, \quad \beta^\dagger = \text{sh}\theta \alpha + \text{ch}\theta \alpha^\dagger \quad (43)$$

such that ρ_1 becomes a single exponential. This amounts to another stretching of the coordinate $y \rightarrow z$.

- Result

$$\rho_1 = K \exp(-\varepsilon \beta^\dagger \beta) \quad (44)$$

This is the form announced above. The Hamiltonian \mathcal{H}_1 in the exponent describes an oscillator with frequency ε where

$$\coth\left(\frac{\varepsilon}{2}\right) = \sqrt{\frac{a}{a-b}} = \frac{1}{2} \left[\sqrt{\frac{\omega_1}{\omega_2}} + \sqrt{\frac{\omega_2}{\omega_1}} \right] \quad (45)$$

and its eigenfunctions are those quoted in the Schmidt decomposition (16) when expressed in terms of x_1 .

This derivation can be generalized to any number of oscillators in a larger system, which proves the general statement for this case. However, one sees that the calculation involves a number of steps and is already somewhat tedious for the simple case treated above. It is therefore fortunate that another much simpler approach exists which we will discuss for fermions [14, 15].

2.4. Method 2 - Correlation functions

Consider a system of free fermions hopping between lattice sites with Hamiltonian (36). The ground state is a Slater determinant describing the filled Fermi sea. In such a state, all many-particle correlation functions factorize into products of one-particle functions. For example,

$$\langle c_m^\dagger c_n^\dagger c_k c_l \rangle = \langle c_m^\dagger c_l \rangle \langle c_n^\dagger c_k \rangle - \langle c_m^\dagger c_k \rangle \langle c_n^\dagger c_l \rangle \quad (46)$$

If all sites are in the same subsystem, a calculation using the reduced density matrix must give the same result. But this is guaranteed by Wick's theorem if ρ_α is the exponential of a free-fermion operator

$$\rho_\alpha = K \exp\left(-\sum_{i,j=1}^L h_{i,j} c_i^\dagger c_j\right) \quad (47)$$

where i and j are sites in the subsystem. Thus ρ_α is of the type given in (38). The hopping matrix $h_{i,j}$ is then determined such that it gives the correct one-particle correlation functions $C_{i,j} = \langle c_i^\dagger c_j \rangle$. This is done in the common diagonal representation of both matrices.

If $\phi_l(i)$ are the eigenfunctions of \mathbf{C} in the subsystem with eigenvalues ζ_l , the transformation

$$c_i = \sum_l \phi_l(i) f_l \quad (48)$$

makes the one-particle function diagonal in the new operators f_l

$$\langle f_l^\dagger f_{l'} \rangle = \zeta_l \delta_{l,l'} \quad (49)$$

To obtain this by taking the trace with ρ_α , the operator \mathcal{H}_α must have the diagonal form given in (38) with the two eigenvalues related by

$$\varepsilon_l = \ln\left(\frac{1-\zeta_l}{\zeta_l}\right) \quad \text{or} \quad \zeta_l = \frac{1}{e^{\varepsilon_l} + 1} \quad (50)$$

Features

- Derivation is very short and clear
- Valid for any Slater determinant
- Gaussian nature of the problem, only simplest correlator enters
- Similar for bosonic case

2.5. Example

Ring with N sites and nearest-neighbour hopping. The single-particle states are plane waves and H is diagonalized by putting

$$c_n = \frac{1}{\sqrt{N}} \sum_q \exp(iqn) c_q \quad (51)$$

In the ground state, the states are filled up to q_F and the correlation function is

$$C_{m,n} = \frac{1}{N} \sum_q \exp(-iq(m-n)) \langle c_q^\dagger c_q \rangle \quad (52)$$

$$= \int_{-q_F}^{q_F} \frac{dq}{2\pi} e^{-iq(m-n)}, \quad N \rightarrow \infty \quad (53)$$

$$= \frac{\sin(q_F(m-n))}{\pi(m-n)} \quad (54)$$

Due to the translation invariance, it depends only on the difference $m - n$. For half filling $q_F = \pi/2$. Note the oscillation and the power-law decay of the correlations corresponding to a *critical* system. Mathematically, it is a sort of Hilbert matrix.

Choose a segment of L consecutive sites as subsystem, diagonalize the matrix numerically and order the eigenvalues according to their magnitude. This gives the following fig. 4.

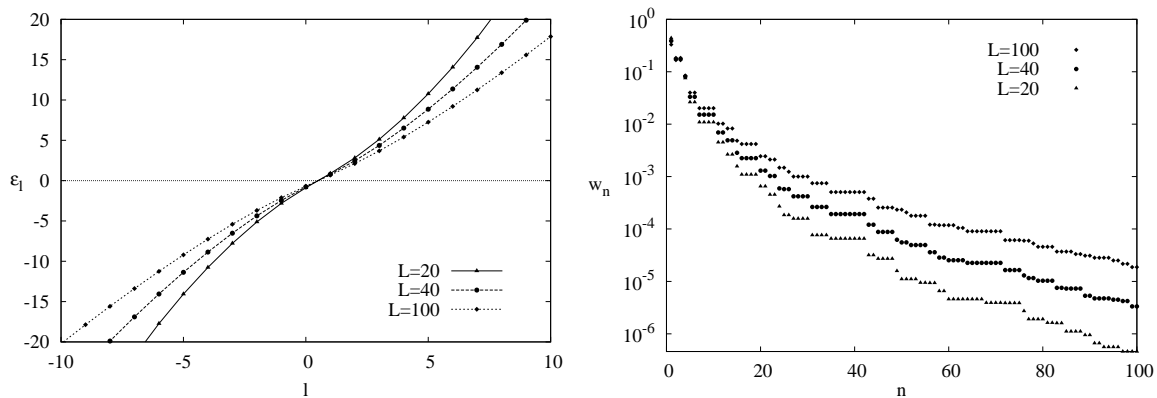


Figure 4. Density-matrix spectra for a segment of L sites in an infinite hopping model. Left: Single-particle eigenvalues ϵ_l . Right: Total eigenvalues w_n . From [16]. Copyright Springer-Verlag, reprinted with permission.

Features

- Dispersion of ε_l roughly linear with curvature
- Values of order 1 and larger
- Curves flatter for larger L
- Rapid initial decrease of the w_n
- Entanglement small, but increasing with L

2.6. Characteristics of the problem

(a) Single-particle eigenfunctions

For the low-lying ε_l , the eigenfunctions are localized near the boundaries.

This is shown in fig. 5 for a non-critical and a critical hopping chain.

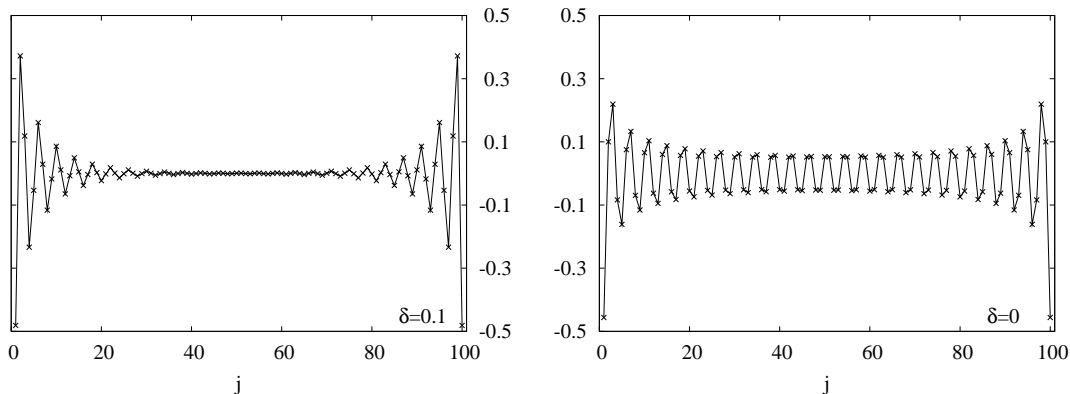


Figure 5. Lowest lying single-particle eigenstates in a dimerized ($\delta = 0.1$, left) and a homogeneous ($\delta = 0$, right) hopping model for a segment of $L = 100$ sites. From [16]. Copyright Springer-Verlag, reprinted with permission.

Consequences

- Double degeneracy of low ε_l for segments in non-critical chains
- Slower decay of the resulting w_n

In fig. 6 this is illustrated for a half-chain of coupled oscillators. Shown are the results both for the open chain (fig. 1 left) where one has one boundary and for the ring (fig. 1 centre) where the subsystem is a segment with two boundaries.

The slower decay of the w_n leads to a poorer performance of the DMRG for rings and explains why the method is normally used in the open-chain geometry. In two dimensions, whole bands of ε_l arise which are associated with the boundary between the subsystems, see section 4.4. In the entanglement entropy this leads to the so-called “area law”.

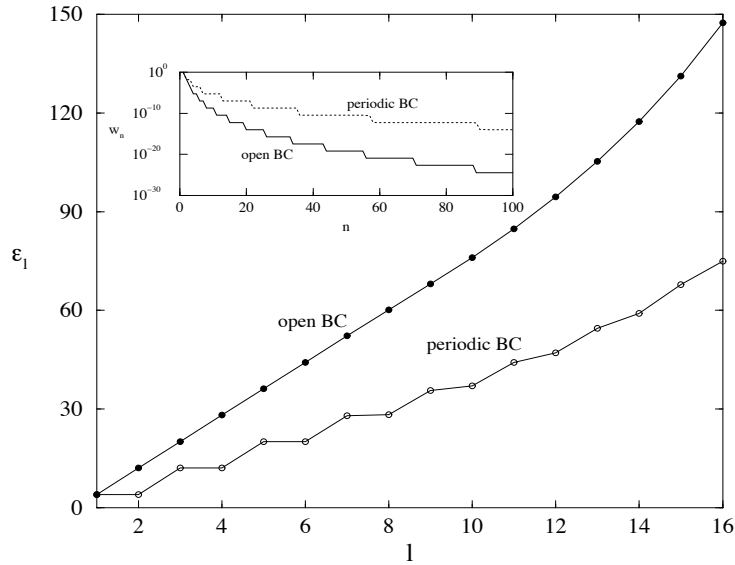


Figure 6. Spectra for one-half of an oscillator chain with $k = 0.5$ and $L = 32$ sites. From Chung [17].

(b) Entanglement Hamiltonian \mathcal{H}_α

In general, this operator is different from the Hamiltonian of the subsystem.

This is shown in fig. 7 for a segment in a hopping chain. The hopping matrix $h_{i,j}$ in (47) was calculated, using the common eigenfunctions ϕ_l of \mathbf{C} and \mathbf{h} , via

$$h_{ij} = \sum_l \phi_l(i) \varepsilon_l \phi_l(j) \quad (55)$$

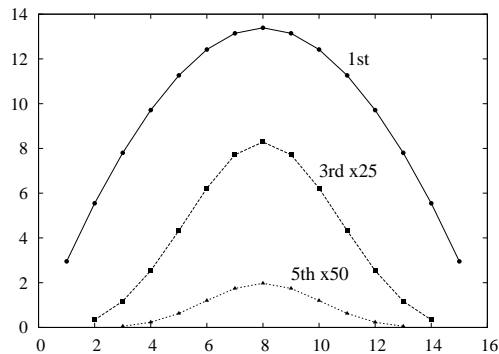


Figure 7. Matrix elements in \mathcal{H}_α for a hopping model. First, third and fifth neighbour hopping in a segment of $L = 16$ sites. From [1]. Copyright IOP Publishing. reprinted with permission.

The dominant elements are those for nearest-neighbour hopping and vary roughly parabolically, whereas in the chain they are constant. For a half-chain one finds half a parabola.

(c) Spectrum of \mathbf{C}

In a large subsystem, most of the eigenvalues ζ_l lie (exponentially) close to 0 and to 1.

This is illustrated in fig. 8 for a segment in a hopping model

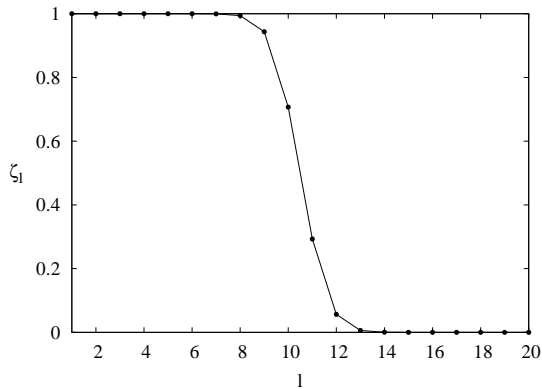


Figure 8. Eigenvalues of the correlation matrix for a segment of $L = 20$ sites in a hopping chain.

It can be understood from (52) as follows

- In the total system, the eigenvalues are $\langle c_q^\dagger c_q \rangle = 0, 1$
- Restricting \mathbf{C} to the subsystem changes the spectrum
- Low-lying states localized near the boundary appear, compare (a)
- But bulk states remain

In numerics, this leads to the following difficulty. The closeness of ζ_l to 0 or 1 soon exceeds the usual double-precision accuracy. The ε_l can then no longer be determined reliably, unless one works with special techniques. Therefore the values of the ε_l in most of the figures shown here do not exceed 20-30. However, for the entanglement this does not matter, since large ε_l give negligible contributions.

A special role is also played by eigenvalues $\zeta_l = 1/2$ corresponding to $\varepsilon_l = 0$. Such an eigenvalue causes a two-fold degeneracy of all w_n and is therefore seen in the RDM spectrum. These zero modes have found much interest recently because they may reflect a symmetry of the real Hamiltonian with boundaries.

2.7. Schmidt form for fermions

The correlation function approach gives the Schmidt spectra in a very easy way. But it is also instructive to derive the Schmidt decomposition directly. This is done in the following way [18].

- Consider a system with N particles. Divide the occupied single-particle states $\psi_q(n)$ into the components

$$\psi_q(n) = \begin{cases} \psi_q^1(n) & : n \in 1 \\ \psi_q^2(n) & : n \in 2 \end{cases} \quad (56)$$

These are neither orthogonal nor normalized in their subsystems.

- Find new states $\chi_l(n)$ such that their components $\chi_l^1(n)$ and $\chi_l^2(n)$ are orthogonal in their subsystems. This is done by diagonalizing the overlap matrices

$$M_{q,q'}^\alpha = \langle \psi_q^\alpha | \psi_{q'}^\alpha \rangle, \quad \alpha = 1, 2 \quad (57)$$

Their eigenvalues are ζ_l and $1 - \zeta_l$ and the new functions have the norms

$$\langle \chi_l^1 | \chi_l^1 \rangle = \zeta_l, \quad \langle \chi_l^2 | \chi_l^2 \rangle = 1 - \zeta_l \quad (58)$$

- Form normalized states via

$$\phi_l^1 = \frac{1}{\sqrt{\zeta_l}} \chi_l^1, \quad \phi_l^2 = \frac{1}{\sqrt{1 - \zeta_l}} \chi_l^2 \quad (59)$$

- Define Fermi operators $a_{\alpha,l}$ for the ϕ_l^α . Then

$$|\Psi\rangle = \prod_{l=1}^N \left[\sqrt{\zeta_l} a_{1,l}^\dagger + \sqrt{1 - \zeta_l} a_{2,l}^\dagger \right] |0\rangle \quad (60)$$

where $|0\rangle$ is the vacuum. This gives the Schmidt decomposition if one multiplies out the product.

Comments

- Instead of the $L \times L$ correlation matrix \mathbf{C} , the $N \times N$ overlap matrix \mathbf{M} appears
- However, the non-trivial eigenvalues ζ_l are the same
- A particle in state χ_l is found with probability ζ_l in part 1 and with probability $1 - \zeta_l$ in part 2
- If $\zeta_l = 0$ the particle is found only in subsystem 2. This *has* to happen, if subsystem 1 cannot accomodate all the N particles.
- The approach can be applied to continuous systems where $\psi_q(n) \rightarrow \psi_q(x)$

The approach shows that the single-particle eigenvalues ζ_l in one subsystem are associated with the eigenvalues $1 - \zeta_l$ in the other. The two lead to $\pm\varepsilon_l$ and give the same w_n -spectrum, as it should be.

Example [19]

N free fermions on a ring of length L , subsystem segment $(-\ell/2, \ell/2)$.

Single-particle wavefunctions

$$\psi_q(x) = \frac{1}{\sqrt{L}} \exp(iqx), \quad q = \frac{2\pi}{L}n, \quad n = 0, \pm 1, \pm 2, \dots \quad (61)$$

Overlap matrix in subsystem

$$M_{q,q'}^1 = \langle \psi_q^1 | \psi_{q'}^1 \rangle \quad (62)$$

$$= \frac{1}{L} \int_{-\ell/2}^{\ell/2} dx \exp(-i(q - q')x) \quad (63)$$

$$= \frac{2}{(q - q')L} \sin((q - q')\ell/2) \quad (64)$$

Writing $q = 2\pi m/L$, $q' = 2\pi n/L$, the matrix becomes

$$M_{m,n}^1 = \frac{\sin((\pi\ell/L)(m-n))}{\pi(m-n)} \quad (65)$$

This is the correlation matrix result (54) with the substitution $q_F \rightarrow \pi\ell/L$. The case $\ell = L/2$ corresponds to half filling, and one can take over the lattice results for the ζ_L . Choosing a different segment of the same length changes \mathbf{M} but not the eigenvalues.

2.8. Some additional details

- In the correlation function approach, the eigenvalue equation can also be written in the form

$$(\mathbf{1} - 2\mathbf{C}) \phi_l = \tanh\left(\frac{\varepsilon_l}{2}\right) \phi_l. \quad (66)$$

- If the expectation values $F_{i,j} = \langle c_i^\dagger c_j^\dagger \rangle$ and $F_{i,j}^* = \langle c_j c_i \rangle$ are non-zero, they have to be included in the considerations. Then for real F the equation becomes

$$(2\mathbf{C} - \mathbf{1} - 2\mathbf{F})(2\mathbf{C} - \mathbf{1} + 2\mathbf{F}) \phi_l = \tanh^2\left(\frac{\varepsilon_l}{2}\right) \phi_l. \quad (67)$$

- Instead of working with the usual fermions, one can use Majorana fermions defined by

$$a_{2n-1} = (c_n + c_n^\dagger), \quad a_{2n} = i(c_n - c_n^\dagger) \quad (68)$$

and form the $2L \times 2L$ correlation matrix $\langle a_m a_n \rangle$ in the subsystem. It has eigenvalues $1 \pm i \tanh(\varepsilon_l/2)$. This is usually done if the ‘‘anomalous’’ correlation functions $F_{i,j}$ exist.

- For coupled oscillators, the correlation functions of position variables and of momenta, $X_{i,j} = \langle x_i x_j \rangle$ and $P_{i,j} = \langle p_i p_j \rangle$, take the place of the Majorana variables. The single-particle eigenvalues then follow from

$$2\mathbf{P} 2\mathbf{X} \phi_l = \coth^2\left(\frac{\varepsilon_l}{2}\right) \phi_l. \quad (69)$$

For the two coupled oscillators treated in section 2.3, one has $\langle x_1^2 \rangle = (1/\omega_1 + 1/\omega_2)/4$ and $\langle p_1^2 \rangle = (\omega_1 + \omega_2)/4$ which gives again (45).

3. Integrable models

In one dimension one can exploit the relations between quantum spin chains and two-dimensional classical models. For *non-critical* integrable models, this allows to determine the RDM's and their spectra analytically for *large* systems divided in the middle.

3.1. Transverse Ising model

We will discuss the the approach for the Ising model in a transverse field (TI model) with Hamiltonian

$$H = - \sum_n \sigma_n^x - \lambda \sum_n \sigma_n^z \sigma_{n+1}^z, \quad (70)$$

The transverse field has been set to $h = 1$. The ground state is non-degenerate for $\lambda < 1$ and asymptotically degenerate with long-range order for $\lambda > 1$. If rewritten in terms of Fermi operators, H becomes a quadratic form

$$H = - \sum_n (2c_n^\dagger c_n - 1) - \lambda \sum_n (c_n^\dagger - c_n)(c_{n+1}^\dagger + c_{n+1}). \quad (71)$$

Therefore, according to section 2

$$\rho_\alpha = \frac{1}{Z} e^{-\mathcal{H}_\alpha}, \quad \mathcal{H}_\alpha = \sum_{l=1}^L \varepsilon_l f_l^\dagger f_l \quad (72)$$

and the ε_l could be calculated numerically using the correlation functions. The present approach will give them analytically.

3.2. Relation to a 2D partition function

The TI model has the following features

- H commutes (up to boundary terms) with a particular (diagonal) transfer matrix T of an isotropic 2D Ising model on a square lattice
- Its ground state $|\Psi\rangle$ is the eigenstate of T with maximal eigenvalue

From the second property, it follows that one can obtain $|\Psi\rangle$ from an initial state $|\Psi_s\rangle$ via

$$|\Psi\rangle \sim \lim_{n \rightarrow \infty} T^n |\Psi_s\rangle \quad (73)$$

In this way, one has related $|\Psi\rangle$ to the *partition function* of a two-dimensional semi-infinite Ising strip. This is a discrete path-integral representation of $|\Psi\rangle$. It follows that

- $\rho = |\Psi\rangle\langle\Psi|$ is given by two such strips
- ρ_α is obtained by tying the two half-strips together

In this way, ρ_α is expressed as the partition function of a fully infinite strip with a perpendicular cut. This is shown in Fig. 9 on the left.

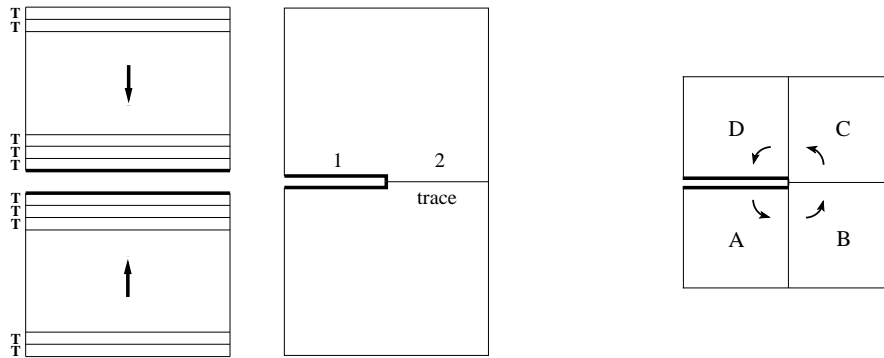


Figure 9. Left: Density matrices for a quantum chain as two-dimensional partition functions. Far left: Expression for ρ . Half left: Expression for ρ_1 . The matrices are defined by the variables along the thick lines. Right: Two-dimensional system built from four quadrants with corresponding corner transfer matrices A, B, C, D . The arrows indicate the direction of transfer. From [16]. Copyright Springer-Verlag, reprinted with permission.

3.3. Some transfer matrix formulae

Before we discuss the evaluation of this particular partition function, we list a few relations for conventional Ising transfer matrices.

(a) One dimension

Consider the Ising chain with Hamiltonian

$$H = -J \sum_n \sigma_n \sigma_{n+1}, \quad (74)$$

where $\sigma_n = \pm 1$. To calculate a partition function, one needs ($K = \beta J$)

$$\begin{aligned} \exp(-\beta H) &= \exp(K\sigma_1\sigma_2) \exp(K\sigma_2\sigma_3) \exp(K\sigma_3\sigma_4) \dots \\ &= T(\sigma_1, \sigma_2) T(\sigma_2, \sigma_3) T(\sigma_3, \sigma_4) \dots \end{aligned} \quad (75)$$

Each T contains the Boltzmann factor for one bond and is a 2×2 matrix

$$T = \begin{pmatrix} e^K & e^{-K} \\ e^{-K} & e^K \end{pmatrix} \quad (76)$$

Summing over all $\sigma_n = \pm 1$ multiplies the matrices together and gives, for a ring of N sites, the partition function $Z = \text{tr } T^N$. In operator form, T can be written

$$T = C \exp(K^* \sigma^x) \quad (77)$$

with the so-called dual coupling K^* defined by $\sinh 2K^* = 1/\sinh 2K$. It is large, if K is small and vice versa.

(b) Two dimensions

In two dimensions, one can build up a lattice row by row. The transfer matrix then contains the Boltzmann factors for the vertical and horizontal bonds in one row. This is shown in fig. 10 (a) by the thick lines.

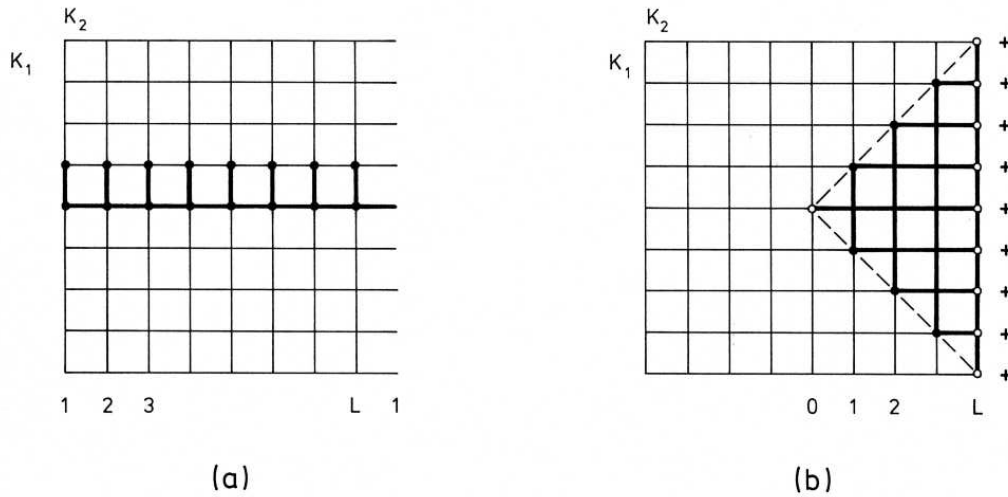


Figure 10. Geometry for two types of transfer matrices. (a) Row-to-row transfer matrix (b) Corner transfer matrix.

For N sites in a row, T is now a $2^N \times 2^N$ matrix and in operator form given by

$$T = T_1 T_2 = C^N \exp\left(K_1^* \sum_n \sigma_n^x\right) \exp\left(K_2 \sum_n \sigma_n^z \sigma_{n+1}^z\right) \quad (78)$$

where K_1 and K_2 are the vertical and horizontal couplings, respectively.

Features

- Terms like in transverse Ising model
- However, the exponentials do not commute
- Exception: $K_1^*, K_2 \ll 1$, strong vertical and weak horizontal bonds. Then one can combine the exponentials. This is called the “Hamiltonian limit”.

3.4. Corner transfer matrices

To calculate the partition function needed for ρ_α , a kind of “circular” transfer matrix would be appropriate. This is indicated in fig. 9 on the right. Then ρ_α would be given by

$$\rho_\alpha \sim ABCD \quad (79)$$

It so happens that such quantities were introduced by Baxter in 1976, see [20]. It turned out that for integrable models they have fascinating and simple properties which make them a powerful tool for calculating order parameters.

(a) *Structure*

In fig. 10 (b) a quadrant of a square lattice model is shown. The CTM contains all Boltzmann factors indicated by thick lines. The internal variables are summed. In operator form, leaving out the prefactor C

- Horizontal bonds
 $\exp(K_2 \sigma_0^z \sigma_1^z)$ (1), $\exp(K_2 \sigma_1^z \sigma_2^z)$ (3), $\exp(K_2 \sigma_2^z \sigma_3^z)$ (5), ...
- Vertical bonds
 $\exp(K_1^* \sigma_1^x)$ (2), $\exp(K_1^* \sigma_2^x)$ (4), $\exp(K_1^* \sigma_3^x)$ (6), ...
- All matrices to be multiplied in correct order from bottom to top

Hamiltonian limit

$$A = e^{-\mathcal{H}_{CTM}} \quad (80)$$

with

$$\mathcal{H}_{CTM} = K_1^* \sum_{n \geq 1} 2n \sigma_n^x + K_2 \sum_{n \geq 1} (2n - 1) \sigma_n^z \sigma_{n+1}^z \quad (81)$$

Features

- Inhomogeneous TI Hamiltonian
- Fields and couplings increase linearly
- Eigenvalues equidistant for $L \rightarrow \infty$

$$\varepsilon_l = \begin{cases} (2l - 1)\varepsilon & , \quad K_1^* < K_2 \\ 2l\varepsilon & , \quad K_1^* > K_2 \end{cases} \quad (82)$$

- To be seen directly in the limiting cases
- Otherwise result of a fermionic calculation

(b) *General case*

So far only the Hamiltonian limit has been considered. The structure of \mathcal{H}_{CTM} is then a consequence of the wedge-like geometry. However, for determining ρ_α via (79), this is not enough, since in the next quadrant the anisotropy is the other way around.

Amazingly, however, the following holds asymptotically

- The eigenvalue spectrum of \mathcal{H}_{CTM} has the form (82) for *arbitrary* couplings
- In the product $ABCD$, the parameter ε which gives the level spacing is

$$\varepsilon = \pi I(k')/I(k), \quad (83)$$

where k with $0 \leq k \leq 1$ is either given by $k = \sinh 2K_1 \sinh 2K_2$ or by $k = 1/\sinh 2K_1 \sinh 2K_2$, whichever is smaller than 1. $I(k)$ is the complete elliptic integral of the first kind and $k' = \sqrt{1 - k^2}$.

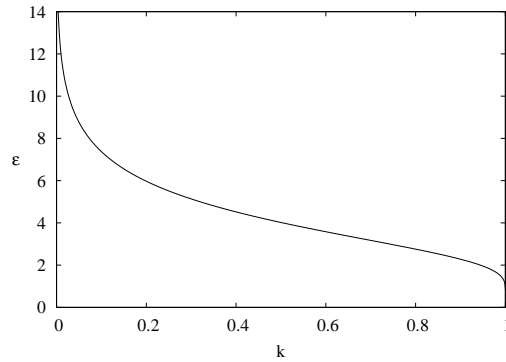


Figure 11. Level spacing as a function of the parameter k . From [1]. Copyright IOP Publishing, reprinted with permission.

The parameter ε diverges for $k \rightarrow 0$ and vanishes for $k \rightarrow 1$, in both cases logarithmically. It is shown in fig. 11.

The *derivation* uses the integrability of the model, which is contained in the so-called star-triangle equations, and a proper elliptic parametrization of the couplings. This leads to two parameters, the k appearing above which is connected with the temperature, and another parameter u which measures the anisotropy, but does not enter the product $ABCD$. A brief account can be found in the Les Houches lectures of Cardy 1988 [21].

(c) *Application to RDM*

The CTM discussed so far can be used for calculating the spontaneous magnetization as expectation value of the central spin. This is sketched in the supplement. However, this central spin is an obstacle for the RDM application, because it is common to all four CTM's and prevents the division of the system into two parts. To calculate the partition function for ρ_α , one uses the modified CTM shown in fig. 12. This amounts to an interchange of the coefficients $2n$ and $2n - 1$ in (81),(82).

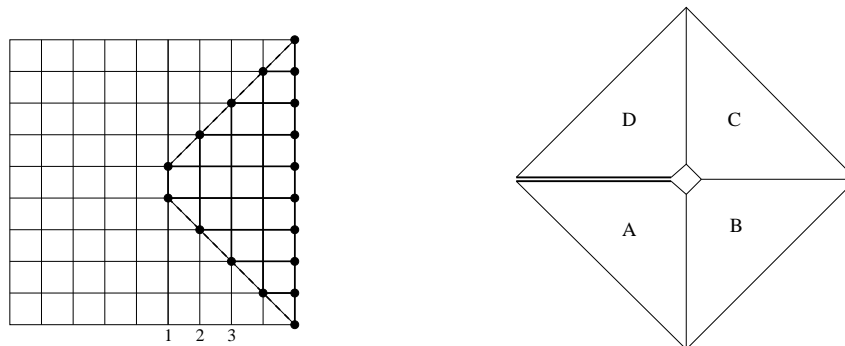


Figure 12. Corner transfer matrices without central spin for calculating the RDM. Left: single matrix. Right: arrangement of four such matrices giving ρ_α .

Summing up, the result for the single-particle eigenvalues in \mathcal{H}_α is

$$\varepsilon_l = \begin{cases} (2l + 1)\varepsilon & , \text{ disordered region} \\ 2l\varepsilon & , \text{ ordered region} \end{cases} \quad (84)$$

where $l = 0, 1, 2, \dots$ and ε is given by (83). In terms of the TI model, the parameter k is

$$k = \begin{cases} \lambda & , \lambda < 1 \\ 1/\lambda & , \lambda > 1 \end{cases} \quad (85)$$

3.5. Spectra and entanglement

In Fig. 13, spectra are shown for a *finite* open TI chain with $N = 20$ sites, divided in the middle. Thus the subsystem has $L = 10$ sites and there are 10 eigenvalues ε_l . The example displays both the infinite-size properties and the modifications by the finite size.

Features

- Linear behaviour of ε_l as predicted
- Deviations at upper end closer to the critical point $\lambda = 1$
- At $\lambda = 1$ shape as for hopping model
- w_n decrease extremely rapidly for small λ (note the scale)
- w_n -decay slower near criticality, but still impressive

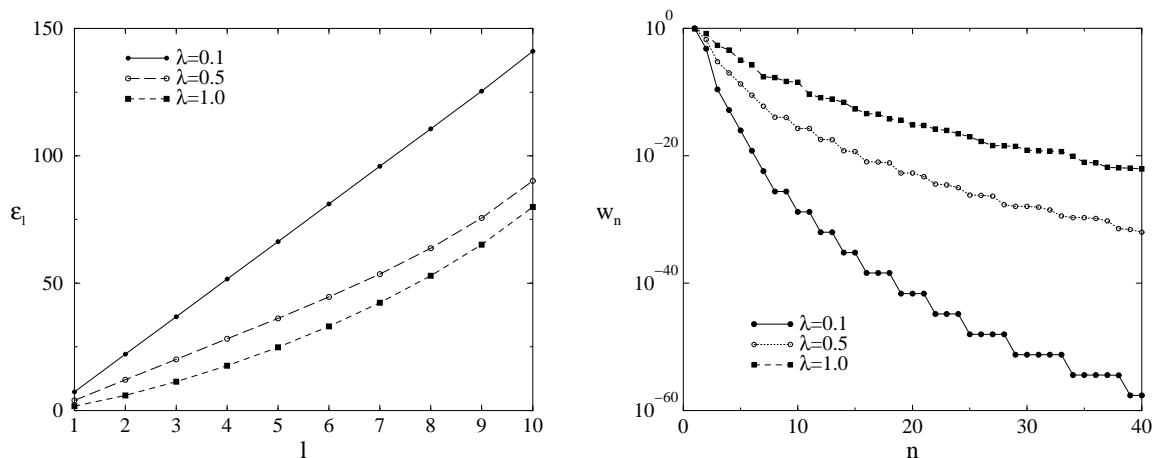


Figure 13. Density-matrix spectra for one-half of a transverse Ising chain with $N = 20$ sites in its ground state. Left: All ten single-particle eigenvalues ε_l . Right: The largest total eigenvalues w_n . From Chung [17].

This means that the ground state is weakly entangled. A Schmidt decomposition can be truncated safely after about 10 terms and this is the explanation for the fantastic performance of the DMRG in this case [22]. Note that altogether there are $2^{10} = 1024$ w_n already in this small system !

Behaviour of the w_n

- Plateaus in w_n for strictly equidistant levels
- Behaviour for large n from number of partitions

$$w_n \sim \exp[-a(\ln n)^2] \quad (86)$$

where $a = \varepsilon 6/\pi^2$.

The case of a segment cannot be treated by the CTM method, but one can simply include the degeneracy seen numerically (section 2.6) into the CTM results. Segments in free-particle models can be treated by a different method which, however, is more technical and less physical than the CTM approach [23].

3.6. Other systems

The CTM approach works also for a number of other quantum chains, namely

- The XY spin chain with Hamiltonian

$$H = - \sum_n \left[\frac{1+\gamma}{2} \sigma_n^x \sigma_{n+1}^x + \frac{1-\gamma}{2} \sigma_n^y \sigma_{n+1}^y \right] - h \sum_n \sigma_n^z \quad (87)$$

This generalization of the TI chain also corresponds to a free-fermion problem.
2D problem: Ising model on a triangular lattice

- The XXZ and XYZ Heisenberg spin chains which contain fermion interactions.
2D problem: Eight-vertex model
- The oscillator chain with nearest-neighbour coupling.
2D problem: Gaussian model

It turns out that the CTM spectrum has the form (84) for *all* these models, even if they contain interactions. Thus one has a *universality* in these problems which makes the entanglement properties of all the fermionic systems identical. Only the parameter k is related differently to the system parameters in each case. For the oscillator chain, for example, it is given by $k/(1-k)^2 = K/\omega_0^2$ if K is the nearest-neighbour coupling. This chain is the bosonic analogue of the TI chain, but it has no ordered phase. In spite of the different statistics, the w_n spectra are similar and the asymptotic law (86) holds with a smaller a .

The bosonic formula can also be used to treat exactly a *two-dimensional* lattice of coupled oscillators which is divided in the middle by a straight line. This is because by making a Fourier transformation parallel to the interface, the problem separates into uncoupled chains.

3.7. Supplement: Onsager formula

With the CTM spectra for the 2D Ising model, the famous Onsager formula for the spontaneous magnetization can be derived in a few lines. Working in the geometry of

fig. 10 (b) and fixing the outer spins as indicated, the expectation value of the central spin has the form

$$\langle \sigma_0 \rangle = \frac{Z_+ - Z_-}{Z_+ + Z_-} \quad (88)$$

where Z_+ and Z_- are the partition functions with σ_0 parallel and antiparallel to the boundary spins, respectively. In terms of the CTM's, this becomes a quotient of traces

$$\langle \sigma_0 \rangle = \frac{\text{tr}(\sigma_0^z \sigma_L^z ABCD)}{\text{tr}(ABCD)} \quad (89)$$

In the fermionic representation, the operator $\sigma_0^z \sigma_L^z$ can be expressed in terms of the operators which diagonalize \mathcal{H}_{CTM} as $\exp(i\pi \sum_l f_l^\dagger f_l)$. The trace can then be performed for each l separately and the exponential factor leads to a minus sign in the numerator. Thus

$$\langle \sigma_0 \rangle = \prod_l \frac{1 - e^{-\varepsilon_l}}{1 + e^{-\varepsilon_l}} \quad (90)$$

Since one has to consider the ordered region, one has to choose $\varepsilon_l = (2l - 1)\varepsilon$ in (82). With $q = e^{-\varepsilon}$ the product then is

$$\langle \sigma_0 \rangle = \prod_{l=1}^{\infty} \frac{1 - q^{2l-1}}{1 + q^{2l-1}} \quad (91)$$

Due to its definition, q is an elliptic nome and the infinite product in (91) has a simple relation to the elliptic moduli k and k' which appear in ε . This gives

$$\langle \sigma_0 \rangle = (k')^{1/4} = (1 - k^2)^{1/8} \quad (92)$$

which is Onsager's formula. The parameter k is here $k = 1/\sinh 2K_1 \sinh 2K_2$. It is interesting to note that also Yang in his 1952 proof of Onsager's result [24] derived an infinite product equivalent to (91), although his approach was quite different. In the CTM formalism, it appears in a natural way, and also the order parameters for more complicated models take such product forms, see Baxter's book.

4. Entanglement entropies

We have seen already some RDM spectra, which contain the full entanglement information. In this section we want to see how their properties translate into the entanglement entropy. Entanglement entropies are the standard quantities considered in this area and have been the topic of a large number of studies.

4.1. General

Due to the form of the ρ_α , one has the same expressions for the von Neumann entropy as in thermodynamics. Thus, $F = U - TS$ with $T = 1$, or $S = -F + U$, and the free-particle character of \mathcal{H}_α gives, as in statistical physics

$$S = \pm \sum_l \ln(1 \pm e^{-\varepsilon_l}) + \sum_l \frac{\varepsilon_l}{e^{\varepsilon_l} \pm 1} \quad (93)$$

where the upper(lower) sign refers to fermions(bosons). From this formula, one can immediately see some general properties

- Largest contributions come from small ε_l
- Therefore entropy particularly large in critical systems
- Maximum value for fermions $L \ln 2$ if all $\varepsilon_l = 0$
- If all ε_l are m -fold degenerate, S has m times the value without the degeneracy

The last property is an additivity which appears e.g. for uncoupled chains or for two independent interfaces. As to the magnitude, an eigenvalue $\varepsilon_l \sim 1$ also gives a contribution of order 1 to S and the sums converge rapidly for larger ε_l .

4.2. Example: TI chain

With the spectra found in section 3, it is easy to calculate S for the infinite transverse Ising chain. The result of a numerical evaluation is shown in fig. 14

One notes the following features

- S vanishes for $\lambda \rightarrow 0$.
Formally: All ε_l diverge. Physically: $|\Psi\rangle$ becomes product state.
- S goes to $\ln 2$ for $\lambda \rightarrow \infty$.
Formally: All ε_l except one diverge, ε_0 is zero. Physically: $|\Psi\rangle$ is superposition of the two product states $|+++ \dots\rangle$ and $|- - - \dots\rangle$.
- S diverges at the critical point $\lambda = 1$. Formally: $\varepsilon \rightarrow 0$, slope of the dispersion curve goes to zero. Physically: State becomes more and more entangled as the correlation length increases.

Due to the equidistant single-particle levels, one can even calculate S in closed form. In the disordered region, one finds with $k = \lambda$

$$S = \frac{1}{24} \left[\ln \left(\frac{16}{k^2 k'^2} \right) + (k^2 - k'^2) \frac{4I(k)I(k')}{\pi} \right], \quad (94)$$

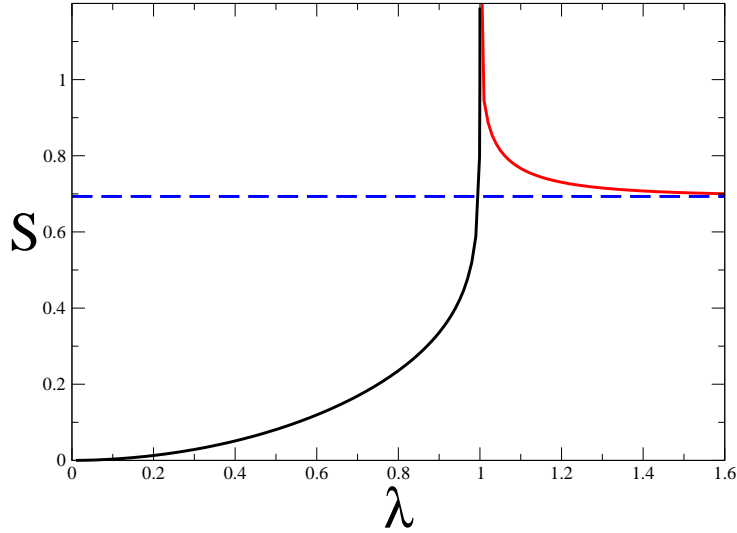


Figure 14. Entanglement entropy between the two halves of an infinite TI chain as a function of λ . From Calabrese and Cardy [25]. Copyright IOP Publishing, reprinted with permission.

A similar expression with an additional contribution of $\ln 2$ coming from the eigenvalue $\varepsilon_0 = 0$ holds in the ordered region.

From this, one can extract the behaviour near $k = 1$

$$S = \frac{1}{12} \ln \left(\frac{8}{1-k} \right) \quad (95)$$

and since the correlation length is given by $\xi \sim 1/(1-k)$, this can be written

$$S = \frac{1}{12} \ln \xi \quad (96)$$

which shows a *logarithmic* critical behaviour. The effective number of states in the Schmidt decomposition, however, has normal power-law behaviour

$$M_{\text{eff}} \sim \xi^{1/12} \quad (97)$$

In this sense, the coefficient of the logarithm is a critical exponent.

The Rényi entropies are

$$S_n = \frac{1}{1-n} \sum_l \ln \frac{(1 + e^{-n\varepsilon_l})}{(1 + e^{-\varepsilon_l})^n} \quad (98)$$

and lead to more complicated closed expressions, but the critical behaviour is analogous

$$S_n = \frac{1}{24} \left(1 + \frac{1}{n}\right) \ln \xi \quad (99)$$

An unusual structure is seen if one looks at the next (subleading) terms in the expansion. One finds that they are of the form $\xi^{-k/n}$ with $k = 1, 2, 3 \dots$, i.e. the powers depend on the Rényi index n which determines the number of windings in the path integral for ρ_α^n [26, 27]. The same phenomenon is encountered for order parameters on such Riemann manifolds.

4.3. Critical chains

At a critical point, one has to work with finite subsystems. The spectra for a hopping model have already been shown in section 2.5, and a marked size dependence was noted. The dispersion curves of the ε_l became flatter with increasing L . This gives an increase of S . From (96) one can already guess that ξ will be replaced by the length of the subsystem, and this is in fact the case. The asymptotic formula is

$$S = \nu \frac{c}{6} \ln L + k \quad (100)$$

Features

- $\nu = 1, 2$ number of contact points between subsystem and the rest
- k non-universal constant (subleading term)
- c central charge, from conformal considerations, $c = 1/2$ for TI model, $c = 1$ for hopping model

This result can be understood for the hopping model as follows. The ε_l curves for small systems are not linear, but show curvature. However, for large L , more precisely for large $\ln L$, one can use a continuum approximation to the eigenvalue equation to derive the formula, for a segment in a chain,

$$\varepsilon_l = \pm \frac{\pi^2}{2 \ln L} (2l - 1), \quad l = 1, 2, 3 \dots \quad (101)$$

Using this in (93) and changing the sums into integrals gives

$$S = \frac{2 \ln L}{\pi^2} \left[\int_0^\infty d\varepsilon \ln(1 + \exp(-\varepsilon)) + \int_0^\infty d\varepsilon \frac{\varepsilon}{\exp(\varepsilon) + 1} \right] \quad (102)$$

and since both integrals equal $\pi^2/12$ one finds

$$S = \frac{1}{3} \ln L \quad (103)$$

In numerical calculations, this logarithmic law can be seen already in relatively small systems, where (101) does not yet hold, but one has approximately $\ln L \rightarrow \ln L + 2.5$ for the first eigenvalues.

The expression for the Rényi entropy follows in the same way by going over to integrals in (98) and gives for a segment

$$S_n = \frac{1}{6} \left(1 + \frac{1}{n}\right) \ln L \quad (104)$$

4.4. Higher dimensions

As mentioned in section 2.6, one finds bands of ε_l in two dimensions. This is illustrated in fig. 15 for a 10×10 square lattice of coupled oscillators, divided into two halves. The vertical coupling was varied and one can see how the plateaus with 10 levels (for 10 uncoupled chains) develop into bands. The states in a band can be indexed by a

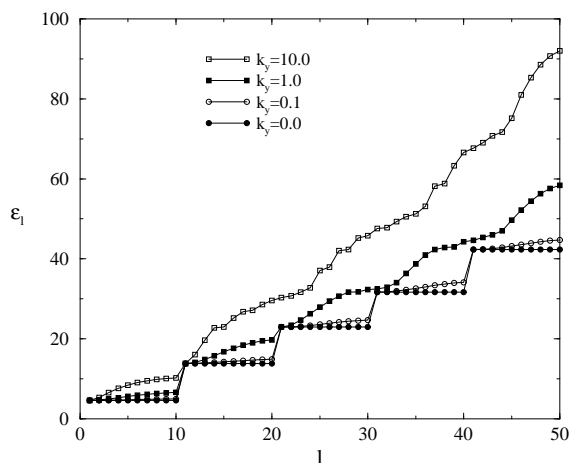


Figure 15. Single-particle eigenvalues for one-half of a 10×10 system of coupled oscillators with $\omega_0 = k_x = 1$ and different couplings k_y . From [28]. Copyright APS, reprinted with permission.

vertical momentum $q_y = q$.

For the entropy, this has the following consequences

- Without coupling: each chain gives the same contribution s to the total entanglement entropy. Thus for M chains one has $S = M s$.
- With coupling: one has to add up the contributions $s(q)$ for each value of q . For large M

$$S = \sum_q s(q) \simeq M \int_0^\pi \frac{dq}{\pi} s(q) \quad (105)$$

- Therefore S proportional to the length of the interface between the subsystems.
- In three dimensions: area of the interface
- Also for other geometries

This is the so-called *area law* for the entanglement entropy. For fermionic critical systems, however, one has logarithmic corrections. For a system with typical size L in d dimensions, one finds

$$S \sim L^{d-1} \ln L \quad (106)$$

if the state corresponds to a finite Fermi surface. This can be proved exactly by putting bounds on S [32, 33], see section 4.7.

4.5. Entanglement across a defect

Since the entanglement is a kind of boundary phenomenon, one expects that it will be changed by a modification of the interface between the subsystems. This has been investigated for hopping chains and critical TI chains with a modified bond, as shown in fig. 16.

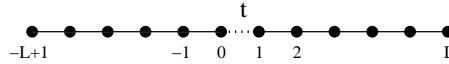


Figure 16. Transverse Ising chain with a bond defect.

Limiting cases

- Chain cut by defect, $t = 0$: no entanglement, $S = 0$
- Chain homogeneous, $t = 1$: logarithmic law (100), $S \sim \ln L$

What happens in between ? Numerical results for the ε_l are shown in fig. 17.

Features

- Development of a gap at the lower end of the spectrum
- Upward shift of the whole dispersion curve as t goes to zero
- Therefore decrease of S for fixed L
- Logarithmic law for S remains valid
- But $c \rightarrow c_{\text{eff}}(t)$.

The variation of c_{eff} with t can be determined numerically, but it turns out that it can also be calculated analytically [29]. Since it is an exercise in going to two dimensions and using partition functions as in section 3, it is presented here briefly. Because one is at the critical point, one can use conformal mappings. The scheme is shown in fig. 18.

In the end, one obtains an expression for the ε_l with a gap which one can insert into the continuum formula (102). The integrals lead to dilogarithms in terms of a parameter $s = 2/(t + 1/t)$ which is the transmission amplitude through the defect, i.e. s^2 is the transmission coefficient. The formula is somewhat long, so it is more instructive to show

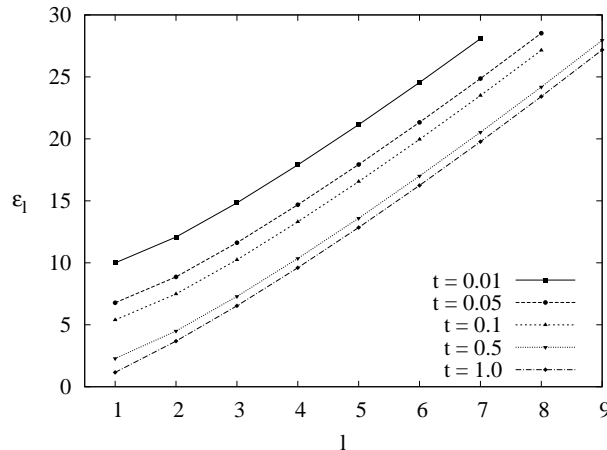


Figure 17. Single-particle eigenvalues ε_l as a function of the defect strength for TI chains with $2L = 300$ sites. From [29]. Copyright Wiley-VCH, reprinted with permission.

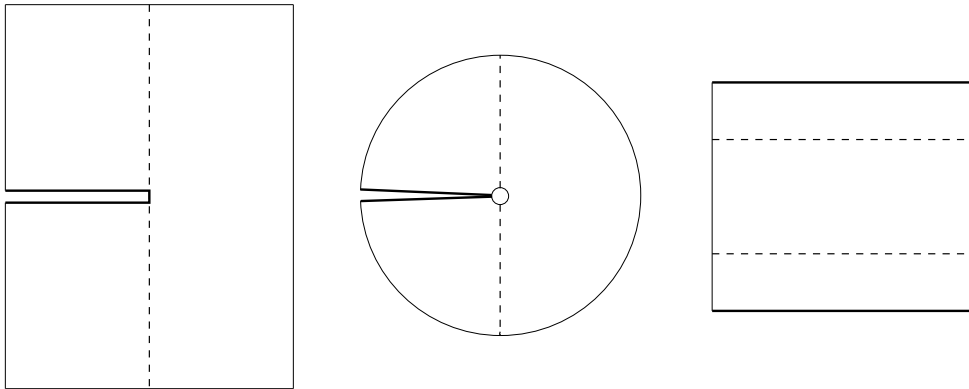


Figure 18. Representation of ρ_α for a chain with a defect in the centre by two-dimensional partition functions. Left: Original representation. Centre: Simplified annular geometry. Right: Strip geometry obtained via the mapping $w = \ln z$. The defect line is always shown dashed. From [29]. Copyright Wiley-VCH, reprinted with permission.

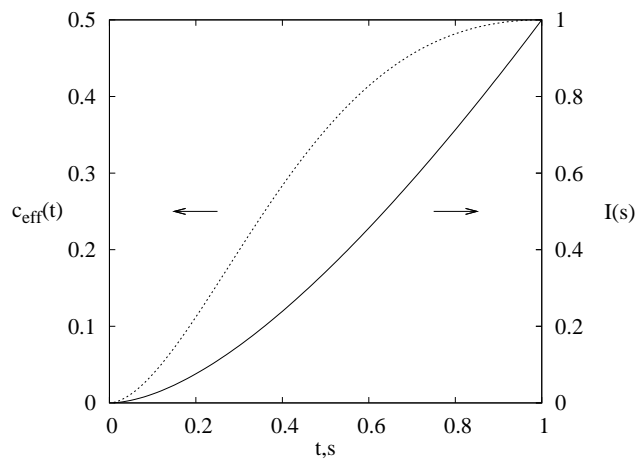


Figure 19. Effective central charge $c_{\text{eff}}(t)$ for a TI chain as a function of the defect strength t (left curve). From [29]. Copyright Wiley-VCH, reprinted with permission.

the result graphically, see fig. 19. For the Rényi entropy S_2 , by the way, one finds a very simple result, namely

$$c_{\text{eff},2} = \frac{8}{\pi^2} \arcsin^2(s/\sqrt{2}) \quad (107)$$

The continuous variation of the coefficient might seem natural, but it is connected with the free-fermion nature of the TI and the hopping chain. The defect is then a “marginal” perturbation which changes also the local magnetic exponent continuously. Things are different for a defect in an XXZ chain, which is a Fermi system with interactions. Then a defect either leads to $c_{\text{eff}} = 0$ if the interaction is repulsive, or is irrelevant, i.e. $c_{\text{eff}} = 1$, if the interaction is attractive. This is in analogy to the transmission properties in this case.

4.6. Inhomogeneous systems

The entanglement can decrease or increase if one makes a system inhomogeneous. This is illustrated here with two simple but instructive examples.

(a) *Hopping chain in a field* [30]

Consider an open chain of $2L$ sites with Hamiltonian

$$H = -\frac{1}{2} \sum_{n=-L+1}^{L-1} (c_n^\dagger c_{n+1} + c_{n+1}^\dagger c_n) + h \sum_{n=-L+1}^L (n - 1/2) c_n^\dagger c_n \quad (108)$$

This describes the so-called Wannier-Stark problem of electrons in a constant electric field. In magnetic language, it is an XX chain with a linearly varying magnetic field in the z -direction. Due to the field, the particles accumulate on the left.

Features

- Density profile, system full on the left and empty on the right
- Characteristic length $\lambda = 1/h$
- Transition region has width 2λ
- Single-particle wave functions are Bessel functions $\phi_k(n) = J_{n-k}(1/h)$, concentrated near site k .
- Single-particle energies are equidistant, $\omega_k = h(k - 1/2)$, Wannier-Stark ladder

Correlation matrix for a half-filled system for $L \rightarrow \infty$

$$C_{mn} = \sum_{k=0}^{\infty} J_{k+m}(\lambda) J_{k+n}(\lambda) \quad (109)$$

$$= \frac{\lambda}{2(m-n)} [J_{m-1} J_n - J_m J_{n-1}] \quad (110)$$

In the limit $\lambda \rightarrow \infty$, this reduces to the result (54) for the homogeneous chain.

The length scale λ is seen also in the low eigenvectors of \mathbf{C} . They are essentially confined to the transition region.

Numerical results for the entanglement entropy if the system is divided in the middle are shown in fig. 20.

Features

- Logarithmic up to $L \approx \lambda$
- Saturation for $L > \lambda$, if $h \neq 0$
- Saturation value for large λ

$$S_\infty(\lambda) = \frac{1}{6} \ln(2\lambda) \quad (111)$$

This is analogous to (96), where the correlation length entered. Interpretation: The parts outside the interface region, which are either full or empty, cannot contribute to the entanglement.

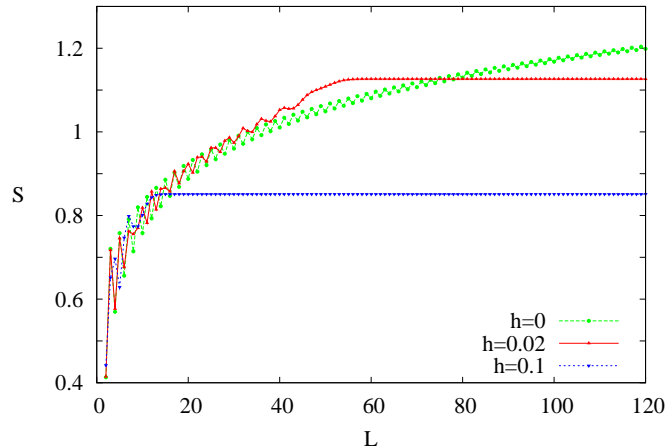


Figure 20. Entanglement entropy for a hopping chain in a linear potential as a function of the half-length L . From [30]. Copyright IOP Publishing, reprinted with permission.

(b) *Inhomogeneous hopping* [31]

Consider a model with Hamiltonian

$$H = -\frac{1}{2} \sum_{n=-L+1}^{L-1} t_n (c_n^\dagger c_{n+1} + c_{n+1}^\dagger c_n) \quad (112)$$

where the hopping amplitudes t_n decay rapidly from the center towards the ends of the chain, for example like $t_n = \exp(-|n|)$. In this model, the density in the ground state is constant as for a homogeneous chain. However, the state is *highly entangled*.

Example: Four sites

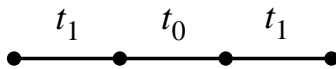


Figure 21. Four-site chain with corresponding hopping amplitudes.

For $t_1 \ll t_0$, the lowest single-particle states have energies $\omega_1 = -t_0$ and $\omega_2 = -t_1^2/t_0$. These states are occupied in the ground state and the corresponding eigenvectors are approximately

$$\phi_1 = \frac{1}{\sqrt{2}} \begin{pmatrix} 0 \\ 1 \\ 1 \\ 0 \end{pmatrix}, \quad \phi_2 = \frac{1}{\sqrt{2}} \begin{pmatrix} 1 \\ 0 \\ 0 \\ -1 \end{pmatrix}, \quad (113)$$

In the first one, sites 2 and 3 are fully entangled, in the second one sites 1 and 4.

The total correlation matrix is

$$\mathbf{C} = \frac{1}{2} \begin{pmatrix} 1 & 0 & 0 & -1 \\ 0 & 1 & 1 & 0 \\ 0 & 1 & 1 & 0 \\ -1 & 0 & 0 & 1 \end{pmatrix} \quad (114)$$

Restricting \mathbf{C} to the left or right half-chain, one finds $\zeta_1 = \zeta_2 = 1/2$, i.e. $\varepsilon_1 = \varepsilon_2 = 0$, which gives $S = 2 \ln 2$. The mechanism persists for larger systems and leads to the concentric structure shown in fig. 22.



Figure 22. Concentric entanglement structure in an inhomogeneous hopping model. After Vitagliano et al. [31].

4.7. Entropy and fluctuations

In hopping models, there is a close connection between the entanglement entropy and the particle-number fluctuations in the considered subsystem. This allows to put bounds on S [32, 33].

In terms of the eigenvalues ζ_l of the correlation matrix \mathbf{C} , one has

$$S = - \sum_l [\zeta_l \ln \zeta_l + (1 - \zeta_l) \ln(1 - \zeta_l)] = \sum_l s(\zeta_l) \quad (115)$$

The function $s(x)$ defined by minus the bracket in (115) has the properties

- Symmetry with respect to $x = 1/2$
- $s(x) = 0$ for $x = 0$ and $x = 1$
- Maximum at $x = 1/2$ with $s(1/2) = \ln 2$

As a result, it can be bounded in $0 \leq x \leq 1$ by a parabola

$$s(x) \geq 4 \ln 2 x(1 - x) \quad (116)$$

and the equality holds for $x = 0, 1/2, 1$. This is shown graphically in fig. 23

It follows that

$$S \geq 4 \ln 2 \sum_l \zeta_l(1 - \zeta_l) = 4 \ln 2 \operatorname{tr}[\mathbf{C}(\mathbf{1} - \mathbf{C})] \quad (117)$$

But the traces can be written as

$$\operatorname{tr}[\mathbf{C}(\mathbf{1} - \mathbf{C})] = \langle N^2 \rangle - \langle N \rangle^2 \quad (118)$$

where $N = \sum_i c_i^\dagger c_i$ is the particle number operator in the subsystem. Therefore the particle-number fluctuations give a lower bound on S

$$S \geq 4 \ln 2 [\langle N^2 \rangle - \langle N \rangle^2] \quad (119)$$

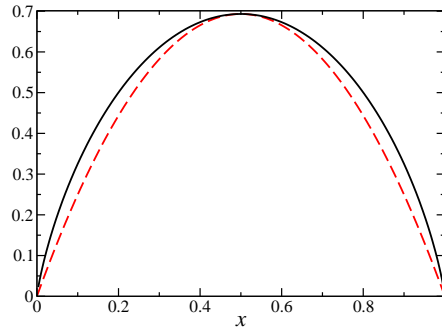


Figure 23. The function $s(x)$ (solid) and its quadratic lower bound (dashed).

These fluctuations have a direct physical significance and are easier to calculate.

Application

- One dimension, large L

$$[\langle N^2 \rangle - \langle N \rangle^2] = \frac{1}{\pi^2} \ln L \quad (120)$$

- Two dimensions, large L

$$[\langle N^2 \rangle - \langle N \rangle^2] \sim L \ln L \quad (121)$$

By shifting the parabola $x(1-x)$ upwards, one can also obtain upper bounds. In this way, one can *prove* the behaviour of the entropy in various dimensions without actually calculating it. The lower bound in 1D gives the prefactor $4 \ln 2 / \pi^2 = 0.28$, which is rather close to the exact value $1/3$. From these considerations, a general formula for the prefactor was obtained which involves an integral over the surface of the subsystem in real space and the Fermi surface in momentum space [33].

5. Quenches and miscellaneous

So far we have been concerned with time-independent situations. In this last section, we turn to cases where the entanglement changes in time. Moreover, I return once more to possible relations between the entanglement Hamiltonian and the real one and finally give a short summary.

5.1. Quenches

If a quantum state changes in time, this will in general affect the entanglement properties. However, the change must be more than a mere phase factor. Thus one has to have a time evolution with a Hamiltonian, for which $|\Psi\rangle$ is not an eigenstate. The simplest set-up is to make an instantaneous change

$$H_0 \rightarrow H_1 \tag{122}$$

After that

- The state $|\Psi\rangle$ evolves as $|\Psi(t)\rangle = e^{-iH_1 t}|\Psi_0\rangle$.
- The total density matrix ρ evolves.
- The RDM's ρ_α also evolve.

If H_1 is a free-particle operator, the arguments work as before. If the initial state was a Slater determinant, the correlation functions at time t

$$\langle\Psi(t)|c_m^\dagger c_n^\dagger c_k c_l|\Psi(t)\rangle = \langle\Psi_0|c_m^\dagger(t)c_n^\dagger(t)c_k(t)c_l(t)|\Psi_0\rangle \tag{123}$$

factor again, because the Heisenberg operators $c_k(t)$ at time t are then linear combinations of the initial ones. Therefore $\rho_\alpha(t)$ has the exponential form (38) but with a time-dependent operator $\mathcal{H}_\alpha(t)$ and the eigenvalues $\varepsilon_l(t)$ follow from the correlation matrix at time t

$$C_{i,j}(t) = \langle\Psi_0|c_i^\dagger(t)c_j(t)|\Psi_0\rangle. \tag{124}$$

Therefore, one only needs to determine the time evolution of the operators $c_j(t)$ in the Heisenberg picture.

Physically, one finds a surprising phenomenon, namely the entanglement *increases* after the quench

- In global quenches $S \sim t$
- In local quenches, $S \sim \ln t$

We show this explicitly for two examples.

5.2. Global quench

Hopping model

- Start from fully dimerized, half-filled model, only pairs of sites $(2n, 2n + 1)$ are coupled and correlated.
- Make it homogeneous with dispersion relation $\omega_q = -\cos q$ and let it evolve.

The time evolution of the Fermi operators then involves Bessel functions

$$c_j(t) = \sum_m i^{j-m} J_{j-m}(t) c_m \quad (125)$$

and the result for the correlation matrix is

$$C_{m,n}(t) = \frac{1}{2} \left[\delta_{m,n} + \frac{1}{2}(\delta_{n,m+1} + \delta_{n,m-1}) + e^{-i\frac{\pi}{2}(m+n)} \frac{i(m-n)}{2t} J_{m-n}(2t) \right] \quad (126)$$

The resulting single-particle spectra are shown on the left of Fig. 30.

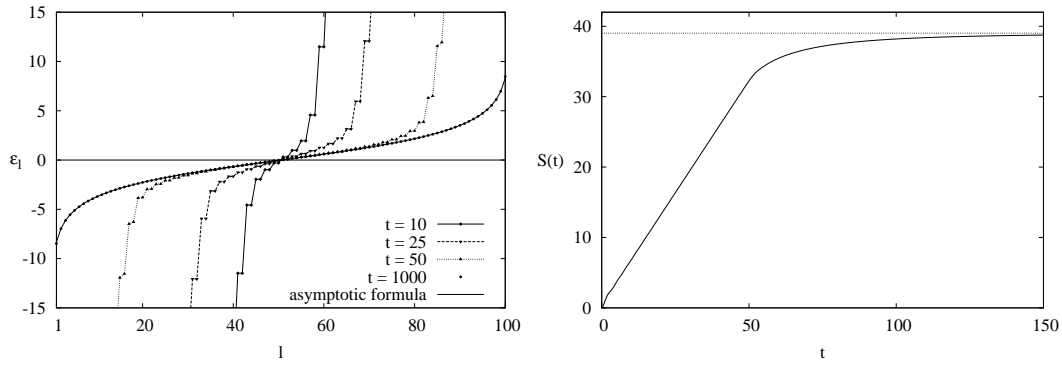


Figure 24. Global quench in a hopping model, starting with a fully dimerized initial state. Left: Time evolution of the single-particle spectrum for a segment of $L = 100$ sites. Right: Entanglement entropy with the asymptotic value. From [30]. Copyright IOP Publishing, reprinted with permission.

Features

- Dispersion linear near zero
- Slope decreases with time, S increases
- For times $t \gg L/2$ approach to a limiting curve, S saturates

The asymptotic form of the spectrum follows from the first three terms in (126) which correspond to a tridiagonal correlation matrix and are the Fourier transform of the constants $\langle c_q^\dagger c_q \rangle$ in the initial state. The eigenvalues for a segment are

$$\zeta_l(\infty) = \frac{1}{2}(1 + \cos q_l), \quad q_l = \frac{\pi}{L+1}l, \quad l = 1, 2, \dots, L \quad (127)$$

and lead to

$$\epsilon_l(\infty) = 2 \ln \tan(q_l/2). \quad (128)$$

The spacing of the q_l is proportional to $1/L$ and gives an *extensive* entropy $S = L(2 \ln 2 - 1)$.

The build-up of an extensive entropy is a typical signature of global quenches.

It has a simple physical interpretation due to Calabrese and Cardy [34] sketched in fig. 25.

- Particle-hole pairs are emitted
- Create entanglement between the subsystem and remainder
- Travel with maximum velocity $v = 1$
- “Light-cone effect”, $S \sim t$ as long as separation $2t < L$

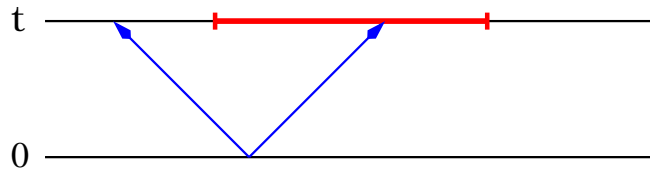


Figure 25. Creation of entanglement after a global quench by emitted particle-hole pairs for the case of a segment in a chain.

The result is relevant for numerical calculations, because it means that one can follow the evolution only for a limited time with DMRG. Beyond that, the state is too entangled to be well approximated.

5.3. Local quench

Hopping model, set-up shown in fig. 26

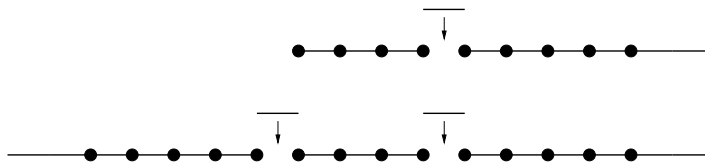


Figure 26. Two variants of a local quench.

- Initially subsystem (center) decoupled from the rest
- Add bond(s) to create a homogeneous chain and let system evolve

The evolution of the Fermi operators is again given by (125), but the initial condition is different. The calculation has to be done numerically. In fig. 27 the result for S is shown.

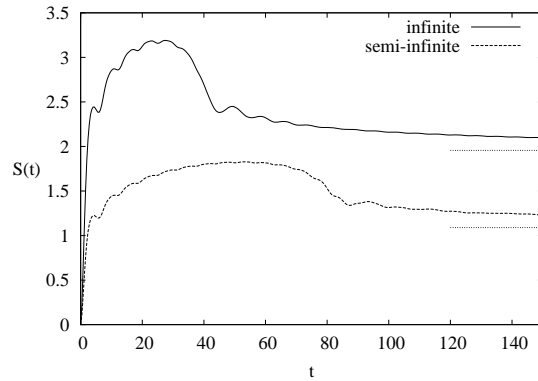


Figure 27. Entanglement entropy for the two geometries after the quench for a subsystem of length $L = 40$. From [36]. Copyright IOP Publishing, reprinted with permission.

Features

- “Entanglement bursts” after the connection
- Duration $t = L$ (infinite case) and $t = 2L$ (semi-infinite case)
- For larger times approach to equilibrium (dotted)

The plateau can be related to a front which starts from the initial defect site and travels through the subsystem until it leaves it again. This is seen directly in the lowest eigenvector in fig. 28. Using methods of conformal field theory, one can derive analytical

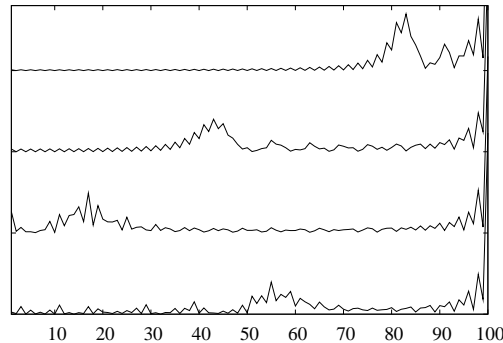


Figure 28. Front propagation in the lowest single-particle eigenvector for the semi-infinite geometry and $L = 100$. Shown are the times $t = 20, 60, 120, 160$. From [36]. Copyright IOP Publishing, reprinted with permission.

formulae for both cases [35, 36]

$$S(t) = \nu \frac{c}{6} \ln \left[\frac{4L}{\nu\pi} t \sin \left(\frac{\nu\pi t}{2L} \right) \right] + k_\nu \quad (129)$$

where ν is the number of contact points and k_ν is a constant which depends on the geometry. This formula is in good agreement with the numerical data. For $t \ll L$, it gives a *logarithmic* entropy growth. If $L \rightarrow \infty$ this persists for *all* times.

For numerical calculations, this is a more favourable situation. One can follow the evolution a much longer time.

5.4. Periodic switching

An interesting effect appears if one connects and disconnects two half-chains periodically for a certain time τ . One can call this a periodic local quench. Numerical results for the entanglement are shown in fig. 29.

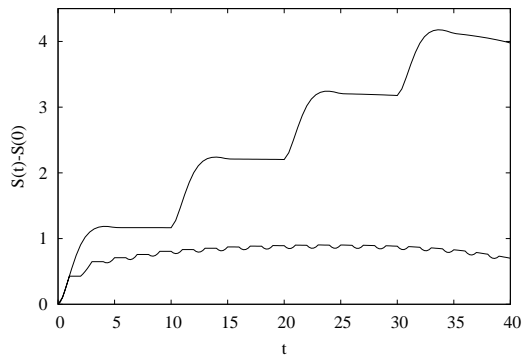


Figure 29. Entropy evolution for periodically connected chains and $L = 40$. Upper curve: $\tau = 5$, lower curve: $\tau = 1$. From [1]. Copyright IOP publishing, reprinted with permission.

Features

- Switching directly visible
- Rapid switching: logarithmic increase
- Slow switching: linear increase

The curve for rapid switching resembles the result for a single quench, compare fig. 27. This can be understood as follows. The time-evolution operator for one period is

$$U = U_0 U_1 = e^{-iH_0\tau} e^{-iH_1\tau} \quad (130)$$

where H_0 and H_1 are the Hamiltonians for the the two configurations and do not commute. However, for small τ , one can take the same Hamiltonian limit as for the transfer matrices in section 3 and combine the exponentials. Then

$$U = e^{-i\bar{H}2\tau} \quad , \quad \bar{H} = \frac{1}{2}(H_0 + H_1) \quad (131)$$

The average time evolution therefore corresponds to a *single* local quench where the final system has a defect with reduced hopping amplitude $t' = t/2$ at the contact. For such a case, the evolution of S is similar as for a quench to a homogeneous system and the behaviour is logarithmic in time.

The curve for slow switching rises on average *linearly*. The interpretation is that here the disconnected system has enough time to “recover” and thereby the

entanglement gain repeats itself after each new connection. The problem can be treated analytically in a continuum model [37].

In general, one can express S in terms of the (time-dependent) cumulants of the probability distribution P_n to transfer n particles. This provides a link to the so-called “full counting statistics” of the junction and thus in principle to measurable quantities. For the example given here, the distribution is Gaussian and only the second cumulant enters.

5.5. Entanglement Hamiltonian and subsystem Hamiltonian

The thermal form of the RDM automatically leads to the question whether there is a relation between \mathcal{H}_α and H_α . In section 2.6 we have already seen that in general this is not so. But are there cases, where a relation exists ?

The answer is yes. For example, it has been seen in Heisenberg ladders, where the subsystem was chosen as one of the two legs. We discuss here an example, which is somewhat simpler and a free-fermion model [38].

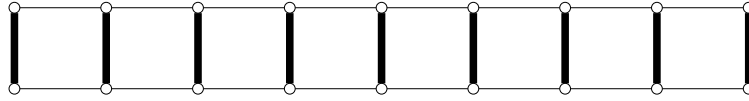


Figure 30. Ladder geometry for a fermionic hopping model. The subsystem is chosen as one of the legs.

Consider a hopping model on a ladder with opposite dispersion in both legs and hopping with amplitude δ between them. The Hamiltonian is

$$H = H_1 + H_2 + H' = \sum_q \gamma_q a_q^\dagger a_q - \sum_q \gamma_q b_q^\dagger b_q + \sum_q \delta (a_q^\dagger b_q + b_q^\dagger a_q) \quad (132)$$

Diagonalizing (132) with a canonical transformation

$$a_q = u_q \alpha_q + v_q \beta_q, \quad b_q = -v_q \alpha_q + u_q \beta_q, \quad u_q^2 + v_q^2 = 1, \quad (133)$$

one obtains

$$H = \sum_q \omega_q (\alpha_q^\dagger \alpha_q - \beta_q^\dagger \beta_q), \quad \omega_q = \sqrt{\gamma_q^2 + \delta^2} \quad (134)$$

From that, one obtains the correlation matrix. Due to the translation invariance, it is diagonal in momentum space and in the subsystem 1 of the a 's one has

$$\zeta_q = \langle a_q^\dagger a_q \rangle = v_q^2 = \frac{1}{2} \left(1 - \frac{\gamma_q}{\omega_q} \right) \quad (135)$$

This gives the single-particle eigenvalues

$$\varepsilon_q = \ln \left(\frac{\omega_q + \gamma_q}{\omega_q - \gamma_q} \right) \quad (136)$$

and \mathcal{H}_1 has the form

$$\mathcal{H}_1 = \sum_q \varepsilon_q a_q^\dagger a_q \quad (137)$$

If now the rung hopping δ is large, one obtains $\varepsilon_q = 2\gamma_q/\delta$ and the relation

$$\mathcal{H}_1 = \frac{2}{\delta} H_1 \quad (138)$$

This is a direct proportionality between the two Hamiltonians.

Remarks

- Holds for dominating rung couplings
- Follows from first-order perturbation theory in $H_1 + H_2$
- Entanglement near maximum $S = L \ln 2$
- Entropy extensive due to long interface

For arbitrary δ , the single-particle energies ε_q and γ_q are not proportional to each other. Therefore the hopping range in \mathcal{H}_1 is in general different from that in H_1 .

5.6. Concluding remarks

I have given an account of the entanglement properties of solvable models, either free particle or integrable, and shown in particular that

- One is lead to a thermodynamic problem
- A particular Hamiltonian enters
- Its spectrum determines the Schmidt weights
- The ground states of homogeneous chains are weakly entangled
- Global quenches lead to strongly entangled states

Almost all considerations had to do with lattice models. These are the systems one studies in numerical investigations motivated by solid state physics or uses in quantum information. They also have the advantage that no divergencies appear in finite geometries.

This does not mean that continuum systems are unimportant. The first calculations of entanglement entropies took place in the context of black-hole theory and thus in a continuum setting. And the use of conformal invariance has not only shown a deeper connection between the various models but also allowed to derive many special results. But that would be a lecture series in its own. Those who are interested can find a lot of material in a special issue of *J. Phys. A* 42 (2009). There, entanglement for free quantum fields is reviewed by Casini and Huerta [39] and within conformal field theory by Calabrese and Cardy [40].

Acknowledgement

I would like to thank Francisco Alcaraz for the invitation to lecture at the school and the International Institute of Physics for its financial support and the hospitality at Natal. I also thank Ming-Chiang Chung, Viktor Eisler and José Hoyos for a substantial number of figures.

References

- [1] Peschel I and Eisler V 2009 *J. Phys. A: Math. Theor.* **42** 504003
- [2] Ekert A and Knight P L 1995 *Am. J. Phys.* **63** 415
- [3] Schrödinger E 1935 *Naturwissenschaften* **23** 807
- [4] Schmidt E 1907 *Math. Annalen* **63** 433
- [5] Schrödinger E 1935 *Proc. Camb. Philos. Soc.* **31** 555
- [6] Kaulke M and Peschel I 1998 *Eur. Phys. J. B* **5** 727
- [7] Han D, Kim Y S and Noz M E 1999 *Am. J. Phys.* **67** 61
- [8] Li H and Haldane F D M 2008 *Phys. Rev. Lett.* **101** 010504
- [9] White S R 1992 *Phys. Rev. Lett.* **69** 2863
- [10] White S R 1993 *Phys. Rev. B* **48** 10345
- [11] Schollwöck U 2005 *Rev. Mod. Phys.* **77** 259
- [12] Lieb E, Schultz T and Mattis D 1961 *Ann. Phys.* **16** 407
- [13] Peschel I and Chung M-C 1999 *J. Phys. A: Math. Gen.* **32** 8419
- [14] Vidal G, Latorre J I, Rico E and Kitaev A 2003 *Phys. Rev. Lett.* **90** 227902
- [15] Peschel I 2003 *J. Phys. A: Math. Gen.* **36** L205
- [16] Peschel I and Eisler V in *Computational Many-Particle Physics* Fehske H, Schneider R and Weisse A, eds 2008 *Lecture Notes in Physics* vol 739 (Berlin: Springer) pp 581-596
- [17] Chung M-C 2002 *Thesis*, Freie Universität Berlin
- [18] Klich I 2006 *J. Phys. A: Math. Gen.* **39** L85
- [19] Calabrese P, Mintchev M and Vicari E 2011 *Phys. Rev. Lett.* **107** 020601
- [20] Baxter R J 1982 *Exactly Solved Models in Statistical Mechanics* (London: Academic Press)
- [21] Cardy J L in *Fields, Strings and Critical Phenomena* Brezin E and Zinn-Justin J, eds 1990 *Les Houches Summer School Session* vol 49 p 169
- [22] Legeza Ö and Fáth G 1996 *Phys. Rev. B* **53** 14349
- [23] Its A R, Jin B-Q and Korepin V E 2005 *J. Phys. A: Math. Gen.* **38** 2975
- [24] Yang C N 1952 *Phys. Rev.* **85** 808
- [25] Calabrese P and Cardy J L 2004 *J. Stat. Mech.* P06002
- [26] Calabrese P, Cardy J and Peschel I 2010 *J. Stat. Mech.* P09003
- [27] Ercolessi E, Evangelisti S, Franchini F and Ravanini F 2011 *Phys. Rev. B* **83** 012402
- [28] Chung M-C and Peschel I 2000 *Phys. Rev. B* **62** 4191
- [29] Eisler V and Peschel I 2010 *Ann. Physik (Berlin)* **522** 679
- [30] Eisler V, Iglói F and Peschel I 2009 *J. Stat. Mech.* P02011
- [31] Vitagliano G, Riera A and Latorre J I 2010 *New J. Phys.* 113049
- [32] Wolf M M 2006 *Phys. Rev. Lett.* **96** 010404
- [33] Gioev D and Klich I 2006 *Phys. Rev. Lett.* **96** 100503
- [34] Calabrese P and Cardy J L 2005 *J. Stat. Mech.* P04010
- [35] Calabrese P and Cardy J L 2007 *J. Stat. Mech.* P10004
- [36] Eisler V, Karevski D, Platini T and Peschel I 2008 *J. Stat. Mech.* P01023
- [37] Klich I and Levitov L 2009 *Phys. Rev. Lett.* **102** 100502
- [38] Peschel I and Chung M-C 2011, Preprint arXiv:1105.3917
- [39] Casini H and Huerta M 2009 *J. Phys. A: Math. Theor.* **42** 504007
- [40] Calabrese P and Cardy J 2009 *J. Phys. A: Math. Theor.* **42** 504005